ION BEAM DEPOSITION OF NITROGEN DOPED DIAMOND-LIKE CARBON THIN FILMS FOR ENHANCED BIOLOGICAL PROPERTIES

A Thesis Submitted to the College of

Graduate Studies and Research

In Partial Fulfillment of the Requirements

For the Degree of Master of Science

In the Department of Mechanical Engineering

University of Saskatchewan

Saskatoon

By

SRINIVASAN SETHURAMAN

Permission to Use

In presenting this thesis in partial fulfillment of the requirements for a Postgraduate degree from the University of Saskatchewan, I agree that the Libraries of this University may make it freely available for inspection. I further agree that permission for copying of this thesis in any manner, in whole or in part, for scholarly purposes may be granted by the professor (Dr. Qiaoqin Yang) who supervised my thesis work or, in her absence, by the Head of the Department or the Dean of the College in which my thesis work was done. It is understood that any copying or publication or use of this thesis or parts thereof for financial gain shall not be allowed without my written permission. It is also understood that due recognition shall be given to me and to the University of Saskatchewan in any scholarly use which may be made of any material in my thesis.

Requests for permission to copy or to make other use of material in this thesis in whole or part should be addressed to:

Head of the Department of Mechanical Engineering

Department of Mechanical Engineering

University of Saskatchewan

57 Campus Drive

Saskatoon, Saskatchewan.

Canada. S7N 5A9.

ABSTRACT

Artificial cardiovascular implants are now made mainly from extruded polytetrafluroethylene (PTFE). However, the limited haemocompatibility of PTFE causes blood clotting and results in early replacement. Many techniques are being developed to improve the haemocompatibility of such devices. One of the most promising techniques is to coat the devices with nitrogen-doped diamond-like carbon (NDLC) thin films. However, the structure of NDLC and its effect on the haemocompatibility of the coated devices have not been fully investigated as required for practical applications. In this thesis, ion beam deposited DLC and Nitrogen doped thin films on PTFE were investigated in order to have a better understanding of the relationships between the structure and biomedical properties of the DLC thin films.

DLC and NDLC thin films were synthesized using ion beam deposition. Commercially available PTFE sheets, which are similar to the material used for vascular grafts, were used as substrates for the DLC thin films. Silicon wafers were also utilized as substrates for condition optimization and property comparison. Raman spectroscopy, atomic force microscopy, X-ray photo emission spectroscopy and scanning electron microscopy were used to study the structural and morphological properties of the coated surface. The results show that the ion beam deposited thin films have a very smooth surface and exhibit low coefficient of friction and high adhesion to the substrate. Low concentration of nitrogen doping in DLC improved surface hardness and reduced surface roughness. Higher concentration of sp^3 hybridized bonds was observed in the DLC thin films on Si than those on PTFE. DLC coating decreased the surface energy and improved the wettability of PTFE films.

The haemocompatibility of the pristine and DLC coated PTFE sheets were evaluated by platelet adhesion technique. The platelet adhesion results showed that the haemocompatibility of DLC coated PTFE, especially NDLC coated PTFE, was considerably improved as compared with uncoated PTFE. SEM observations showed that the platelet reaction on the coated PTFE was minimized as the platelets were much less aggregated and activated.

ACKNOWLEDGEMENTS

I would like to thank Dr. Qiaoqin Yang for giving me the exciting opportunity to carry out this research at the University of Saskatchewan and directing and supervising my work throughout this period of my career. Also, I would like to thank Dr. Thomas Haas, without whom this work would not have been possible. Thanks to Dr. Chris Zhang and Dr. Ike Oguocha who offered many useful pieces of advice and discussions. The training and assistance provided by J. Maley at the Saskatchewan Structural Science Center was valuable for the success of this project.

The author's final acknowledgement and his sincere appreciation go to his wife, daughter, parents, and in-laws for their constant support and encouragement.

The research was funded by Natural Sciences and Engineering Research Council of Canada (NSERC), Canada Research Chair program and a grant from Canada Foundation for Innovation (CFI).

DEDICATION

This work is dedicated to my wife Saradha Srinivasan, daughter Shweta Srinivasan

&

beloved parents Vijayalakshmi and Sethuraman.

TABLE OF CONTENTS

LIST OF TABLES

LIST OF FIGURES

LIST OF ABBREVIATIONS

a-C – Amorphous carbon

a-CN – Amorphous carbon doped with nitrogen

C-N – Carbon nitride films

AFM – Atomic force microscopy

PVD – Physical vapor deposition

COF – Coefficient of friction

CVD – Chemical vapor deposition

CLS – Canadian Light Source

DC – Direct current

DLC – Diamond-like carbon

MSIB – Mass selected ion beam deposition

N-DLC – Nitrogen doped DLC

ePTFE – Expanded polytetrafluoroethylene

IBD – Ion beam deposition

IBAD – Ion Beam Assisted deposition

PTFE – Polytetrafluoroethylene

PLD – Pulsed laser deposition

RIPA – Relative index of platelet adsorption

SEM – Scanning electron microscopy

SGM – Sphercial Grating Monochromator

ta-C – Tetrahedraly-bonded amorphous carbon

TFY – Total fluorescence yield

UMT – Universal Mechanical Tester

XPS – X ray photoelectron spectroscopy

CHAPTER 1

INTRODUCTION

1.1 Motivation

Diamond-like carbon (DLC) thin films exhibit many good properties such as high hardness, high chemical inertness, high wear and corrosion resistance, excellent biocompatibility and very low coefficient of friction, which make this material ideal as protective, corrosion resistant and anti-wear coatings for a variety of applications including bearings, automotive components and biomedical implants (Ali Erdemir *et al*., 2006). There has been keen interest in using various forms of DLC as coatings on artificial hip joints, heart valves, stents and grafts due to their low coefficient of friction and excellent biocompatibility (Geoffrey *et al*., 2005).

Synthesized vascular grafts are now made mainly from extruded polytetrafluroethylene (PTFE). The artificial small-vessels constructed from PTFE are the only alternative to autologous implants for more than 500,000 patients requiring coronary artery bypass surgery and more than 150,000 patients in need of lower limb surgical replacement operations. However, due to their limited haemocompatibility, blood clotting caused by blood-cell adhesion to PTFE becomes a serious problem when the diameter of vascular grafts made from PTFE is less than 6 mm (Srinivasan *et al*., 2008). Thus, one of the most urgent problems to be resolved for wider applications of PTFE vascular grafts, and to avoid the need for patients to undergo repetitive surgery, is to improve heamocompatibility of PTFE-based prosthetic components.

DLC have been demonstrated to be biocompatible *in vitro* and *in vivo* in orthopedic applications. Coating polymer- based biomedical devices such as blood vessels, heart valves, and coronary stents with DLC thin films is expected to significantly improve their haemo, bio-compatibility, tribological performance and lifetime (Narayan, 2005). However, DLC films are always accompanied by a high internal compressive stress due to the ion bombardment during the deposition, which limits their possible applications.

The study of nitrogen doped diamond-like carbon thin films was primarily focused on to synthesize a new form of carbon nitride phase (cubic beta carbon nitride) as proposed by Liu and Cohen, 1990. This phase exhibits higher hardness and bulk modulus than natural diamond. Apart from this, most of the NDLC films deposited so far have been proven to be amorphous in structure. The nitrogen incorporation into DLC in higher percentages has been found to form N-H, C=N and C≡N bonds, which decrease the sp^3 bonds, obstruct the carbon-carbon cross links and form voids resulting in matrix of softer NDLC (Takadoum *et al*., 2003).

Silva *et al.*, 1994 investigated the effects of nitrogen doping on properties of DLC films and showed a clear reduction of the internal compressive stress without significant changes in other properties upon nitrogen doping. Therefore, nitrogen-doped DLC (NDLC) films are more promising to be used as coating on PTFE to improve its haemocompatibility. However, the structure of NDLC and its effect on the haemocompatibility of the coated devices has not been fully investigated as required for practical applications.

1.2 Objective

The objective of this work was to develop ion beam deposition process to synthesize NDLC thin films on PTFE in order to enhance the haemocompatibility of artificial vascular graft made from PTFE.

1.3 Organization of Thesis

The thesis consists of five chapters. Chapter 1 contains an overview of the research motivation and research objectives. Chapter 2 gives a detailed literature review of the structure, the properties, the deposition techniques, the characterization techniques, and the growth mechanism of DLC thin films. Chapter 3 describes the experimental details regarding the deposition and characterization of DLC thin films. The results and discussion of the studies, including the bonding structure, the surface roughness, surface energy and surface morphology, mechanical and biological properties of the coatings, are presented in chapter 4. Chapter 5 provides conclusions drawn from the results, and suggestions for the future work.

CHAPTER 2

LITERATURE REVIEW

2.1 Structure, property and growth of diamond-like carbon thin films

2.1.1 Hybridization and allotropes of carbon

Pure carbon can form different allotropes in various bonding configurations as shown in Figure 2.1. Carbon atoms in diamond have sp^3 hybridization and form four tetrahedral symmetric σ bonds with each other. All carbon bonds are strong and equivalent in diamond. Carbon atoms in graphite have sp^2 hybridization and form trigonal planar configuration, containing both σ and π bonds. The three planar bonds are strong and equivalent. Carbon atoms in many polymers have sp^1 hybridization and linear geometry, containing both σ and π bonds.

Pure carbon usually exists as crystalline structures including diamond and graphite. Carbon also exists as amorphous and nanostructures including C60, carbon nanotubes. Diamond has face-centered cubic crystal lattice as shown in Figure 2.2a. Graphite has hexagonal structure shown in Figure 2.2b. C60 is a perfect ball consisting of sixty carbon atoms with hexagonal and pentagonal rings linked together as shown in Figure 2.2c.

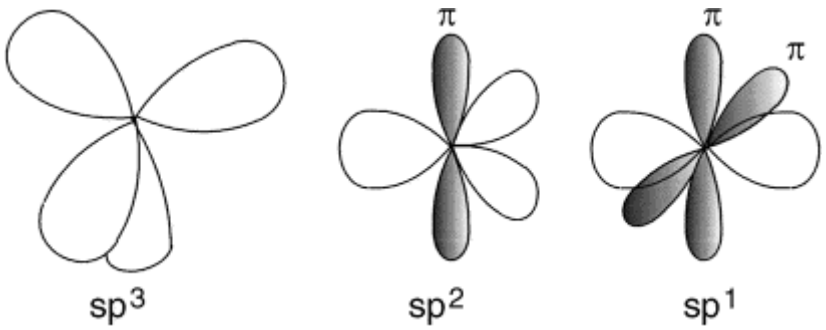

Figure 2.1. Bonding configurations of carbon atom (Robertson, 2002)

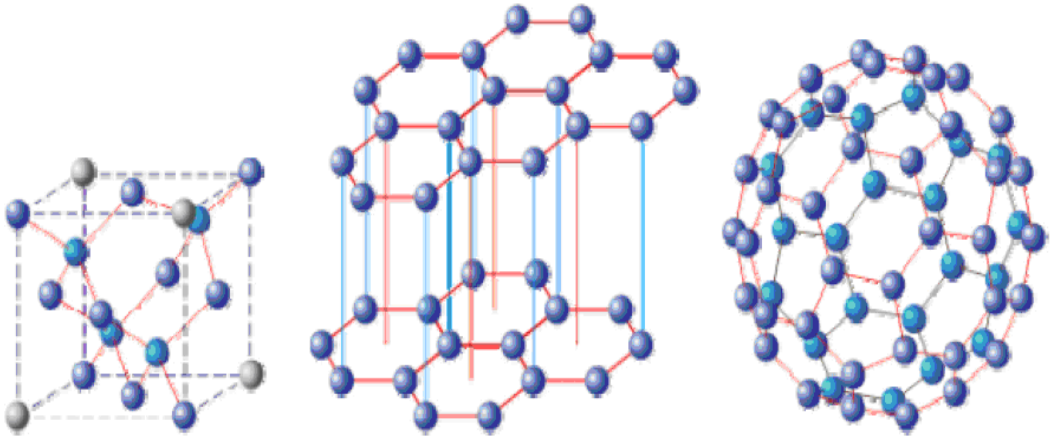

(a) Diamond (b) Graphite (c) C60

Figure 2.2. Carbon allotropes (Foursa, 2007)

Carbon atoms in amorphous carbon materials have no long-range order and may have different hybridizations. Graphite-like amorphous carbon dominates with sp^2-bonded carbon and exhibits properties similar to graphite, whereas diamond-like carbon contains high amount of sp^3 bonded carbon and exhibits properties similar to diamond (Robertson, 1986). Properties exhibited by various forms of carbon are listed in Table 2.1.

Table 2.1. Properties of various forms of carbon (Robertson, 2002)

Material	**Density g/cm^3**	**Band gap(eV)**	**Hardness (GPa)**	**sp^3(%)**	**H (%)**	**Reference**
Diamond	3.515	5.5	100	100	0	Field, 1993
Graphite	2.267	0.0	-	0	0	Kelly, 1981
Glassy carbon	1.3 - 1.55	0.01	3	0	0	Robertson, 1986
Evaporated C	1.9	0.4 - 0.7	3	0	0	Robertson, 1986
Sputtered C	2.2	0.5	1	5	0	Pharr *et al*., 1996
ta-C	3.1	2.5	80	80 - 88	0	Pharr *et al*., 1996
Hard a-C:H	1.6 - 2.2	1.1 - 1.7	10 - 20	40	30 - 40	Koidl *et al*., 1990
Soft a-C:H	1.2 - 1.6	1.7 - 4.0	<10	60	40 - 50	Koidl *et al*., 1990
ta-C:H	2.4	2.0 - 2.5	50	70	30	Weiler *et al*., 1994

2.1.2 Structure and properties of diamond-like carbon

DLC is an amorphous, metastable carbon with high content of sp^3 hybridization. However, its detailed structure has not been completely determined and various models have been proposed with ambiguity in each of them. McKenzie *et al.*, 1983 described DLC as nanocrystalline two-phase structure consisting of polycyclic aromatic hydrocarbon interconnected by tetrahedral carbon. Angus *et al.*, 1991 proposed their model based on a random covalent network (RCN) consisting of sp^3 and sp^2 carbon sites and the ratio of this coordination is a function of atomic fraction of hydrogen in film shown in Figure 2.3. As per Robertson, 1993 the structure of DLC is a network of covalently bonded carbon atoms in different hybridization.

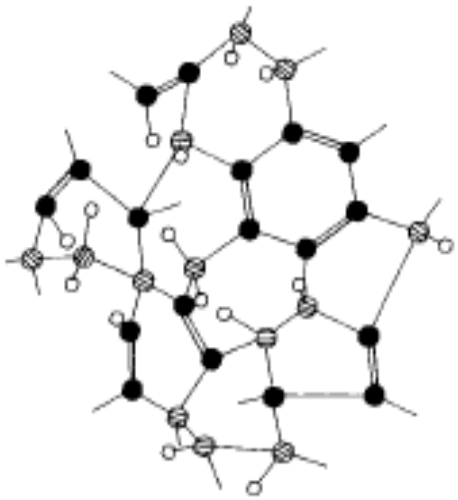

●, sp^2 carbon atom; ◍, sp^3 carbon atom; ○, hydrogen atom.

Figure 2.3. 2-D representation of diamond-like carbon film structure (Angus and Wang, 1991)

Amorphous carbon (a-C) and hydrogenated amorphous carbon (a-C:H) can be categorized into different forms based on the content of hydrogen as shown in Figure 2.4. DLC films usually contain high sp^3 content and are termed tetrahedral amorphous carbon (ta-C) or diamond like hydrogenated amorphous carbon (DLCH) or tetrahedral hydrogenated amorphous carbon (ta-C:H), whereas films with low sp^3 content are termed graphitic C or graphite like hydrogenated carbon (GLCH).

Angus and Hayman, 1988 proposed a classification of hydrogenated amorphous carbon based on the atom number density and hydrogen content as shown in Figure 2.5. DLC films (a-C:H and a-C in Figure 2.5) have much higher atom number density than conventional polymers.

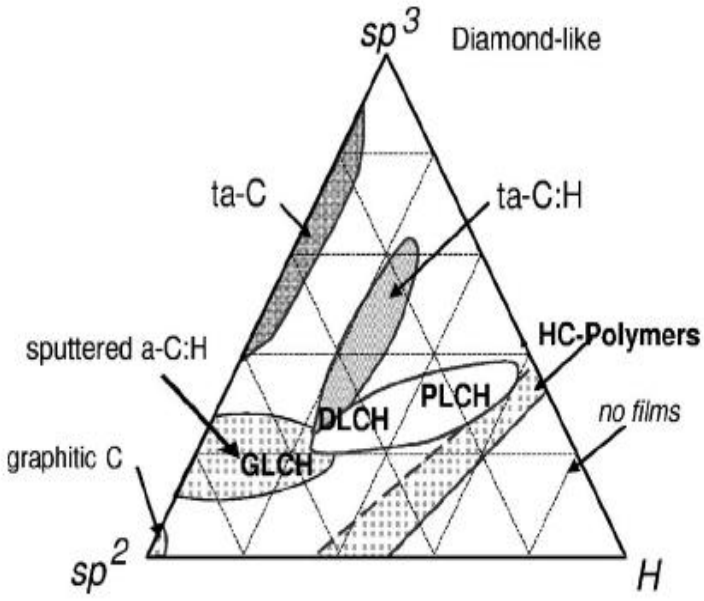

Figure 2.4. Ternary phase diagram showing various forms of DLC (Casiraghi, Ferrari and Robertson, 2005)

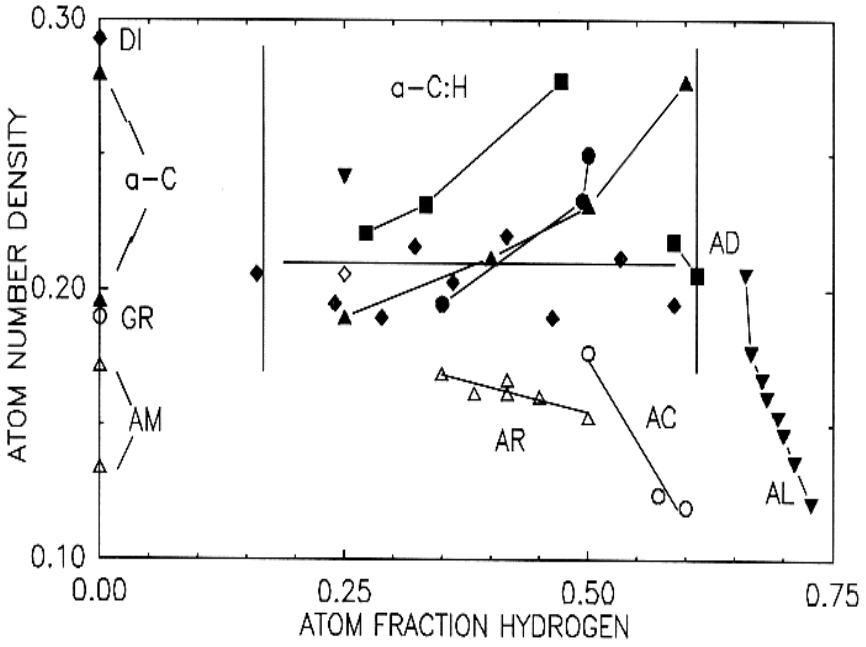

Figure 2.5. Atom number density vs. atom fraction of hydrogen (Angus and Hayman, 1988)

(Expressed in gram atom/cm^3. Symbols used are, AC- oligomers of acetylene, AD- adamantanes, AL –nalkanes, AM- amorphous carbon, AR – polynuclear aromatics, DI - diamond and GR – graphite)

Table 2.2 illustrates the structure, composition and properties of a-C and a-C:H films. As the hydrogen content increases in hydrogenated films, there is a decrease in hardness, Young's modulus, coefficient of friction, compressive stresses, density and refractive index.

DLC's amorphous nature make it feasible to be doped with small amounts of different elements like N, O, F, Si and their combinations to improve and control their mechanical, tribological and biological properties.

Efficiency of doping nitrogen (N) in DLC to form solid solution is very poor. N can take any bonding configuration shown in Figure 2.6. N atoms can occupy sp^3 substitutional sites or sp^2 substitutional sites as a result of doping. They can also form pyridine, pyrrole and nitrile instead of forming solid solution.

The incorporation of nitrogen promotes the formation of pentagonal rings and facilitates cross-linking between the planes (Hellgren *et al.,* 1999), making the films highly elastically deformable and thus improving the toughness of the films. N atoms incorporated into DLC may also form N-H, C=N, C≡N bonds which decrease the sp^3 carbon bond content, obstruct the carbon-carbon links and form voids and result in softer a-C:H:N films (Kusano *et al.*, 1998). High concentration of N up to 34% has been reported to be doped into DLC and the doping reduced the internal stresses without affecting the hardness and wear resistance (Koskinen *et al.*, 1996). However, the work that has been performed in this area is insufficient to develop an in-depth understanding of the effect of nitrogen doping on the structure and properties of DLC.

Table 2.2. Range of DLC structure, composition and properties (Erdemeir, 2001)

Variable	a-C	a-C:H
Hydrogen content, at %	<5	20 - 60
sp^3, %	5 - 90	20 - 65
Density, g/cm^3	1.9 - 3.0	0.9 - 2.2
Thermal stability, C	<600	<400
Optical gap, eV	0.4 - 1.5	0.8 - 4.0
Electrical resistivity, ohm/cm	10^2 - 10^{16}	---
Refraction index	1.8 - 2.4	---
Compressive stress, GPa	0.5 - 5	---
Hardness, GPa	<80	<60
Young's Modulus, GPa	<900	<300

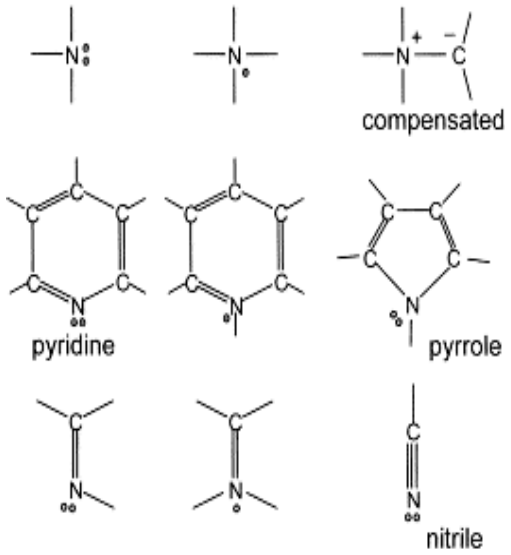

Figure 2.6. Carbon nitrogen bonding configurations(Robertson, 2002)

2.1.3 Deposition of diamond-like carbon thin films

The first successful diamond-like carbon film was synthesized by Aisenberg and Chabot in early 1970. Recently, there is a wide spread interest in developing commercially viable processes for producing DLC thin films. The techniques used to grow DLC include direct current (DC) or radiation frequency (RF) plasma enhanced vapor deposition, sputtering, ion beam deposition, pulsed laser deposition, cathodic arc deposition and ion beam deposition. Each of these processes has its own advantages and disadvantages in terms of deposition rates, quality of films and uniformity. The synthesized thin films have a wide range of structures and properties depending on the deposition conditions.

Plasma enhanced deposition utilizes a glow discharge to activate gas species needed for physical vapor deposition (PVD) or chemical vapor deposition (CVD) processes. Various hydrocarbon gases such as methane, ethane, acetylene, benzene, ethylene and propane were used as carbon source for DLC deposition. The deposited thin films usually consist of hydrogen, thus belong to a-C:H. In sputtering, graphite target sputtered by RF or DC argon plasma, is the carbon source for DLC deposition. The deposited thin films usually consist of pure carbon, and thus belong to a-C category. Magnetron sputtering is commonly used because it increases the path length of electrons and the degree of ionization of plasma, and thus the deposition rate.

In pulsed laser deposition, short intense laser pulses are used to vaporize graphite and to create plasma. The deposited thin films are a-C. However, the ion species and ion energy in all of those techniques have a wide range of distribution and are difficult to be controlled. On contrary, ion beam deposition is a technique where the ion species and ion energy can be well controlled. In

this technique, the precursor's carbon or hydrogenated carbon ions are extracted from the plasma to form an ion beam, and are accelerated to desired ion energy toward substrate at high vacuum, whereas neutrals are filtered and decelerated. This technique provides a highly controlled ion species with controlled energy for DLC deposition, thus the structure and property of deposited DLC thin films are well controlled. Therefore, the use of ion beams for DLC film deposition has been expanding in the past decade.

Ion beam deposition is principally an ion implantation deposition, in which the energetic ion bombardment is used to synthesize high quality films (Xiaoming He *et al.,* 1996). There are different types of ion beam deposition methods as shown in Figure 2.7. They use either solid graphite targets or ionized hydrocarbon gases as carbon source.

As mentioned before, the main advantage of ion-beam deposition process is the high degree control of DLC coating property as a result of the accurate control of critical parameters such as gas flow rate, ion-beam energy and ion beam current. Ion beam deposition also allows for very low temperature growth and simple fixturing. The equipment usually operates at very low pressure, which reduces the potential film contamination. The main limitation with this method is that the hardest films are obtained under conditions of low power and low gas pressure, which results in low deposition rate.

High efficiency ion sources are often employed to make ion-substrate interaction to occur at low pressures of $1*10^{-4}$ torr or less. Operation in high vacuum results in control over fluxes of energetic ion species (Kaufman, 1990).

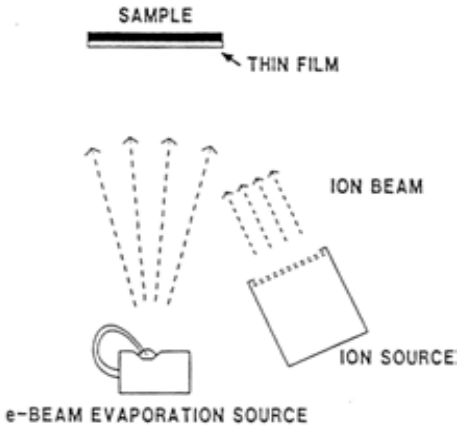

(a)

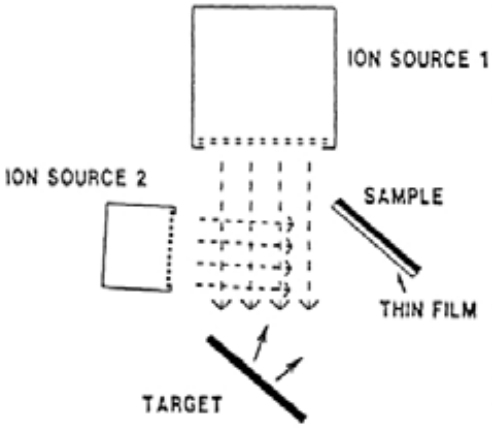

(b)

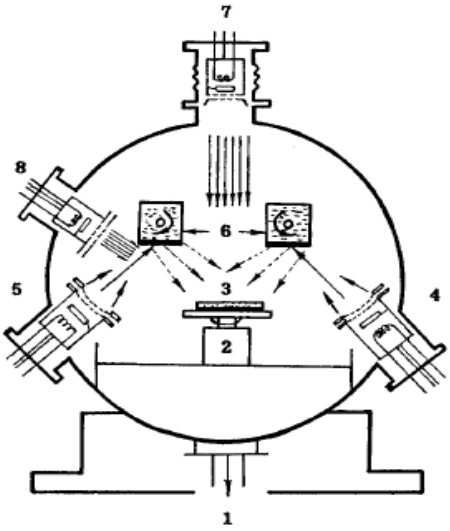

(c)

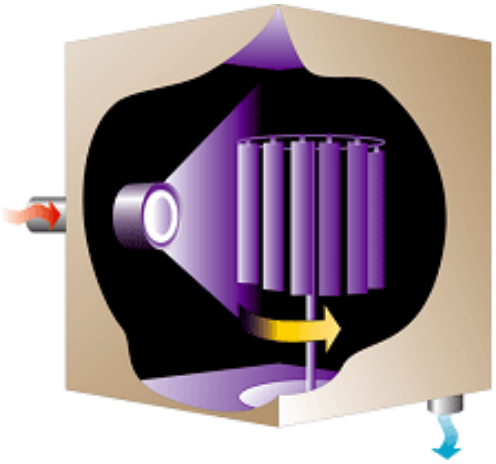

(d)

Figure 2.7. (a) Ion beam assisted EB-evaporation; (b) Ion beam assisted ion beam sputtering; (c) Ion beam assisted dual ion beam sputtering; (d) Ion source (*University of Cambridge-eng.cam.ac.uk*).

2.1.4 Formation processes and mechanisms of diamond-like carbon thin films

1eV of energy corresponds to a temperature of 11,606 K. The impact of ions may enhance surface atom mobility, diffusion, chemical reaction, the formation of metastable phases, and thus modifies the deposited thin films with desired properties. Ion beam at energies of tens of eV usually cause preferential sputtering and thus are used to clean the surface. Ion beams over 40 eV can induce formation of interfacial structure and thus pre-deposition low energy ion bombardment can improve film to substrate adhesion. Ions in the range of 50 – 1000 eV produce lattice movements in the top layer of solids. The motion is isolated and described as non-equilibrium and not steady state. Ions with this moderate energy can also result in shallow implantation into a growing film. However, ions at hundreds of eV energies can also cause significant atomic displacement and damage to the surface below. To minimize the structural damage of the deposited film the ion beams are to be kept at less than 400 eV in direct deposition processes (Aisenberg and F.M.Kimock, 1990). The effect of energetic ion flux on surface atoms is illustrated in Figure 2.8.

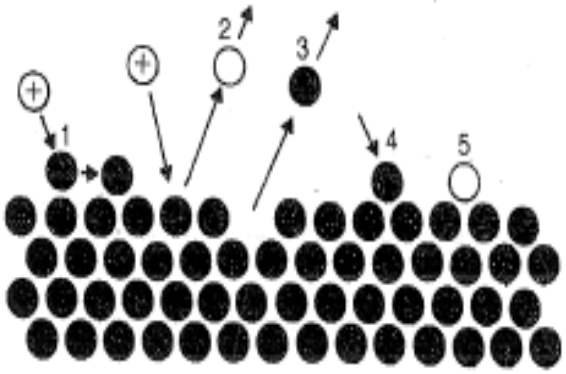

Figure 2.8. Effect of energetic ion flux on surface atoms (Aisenberg and Kimock, 1990)

1. Impinging ions providing energy for lateral motion of surface atom into advantageous site.
2. Sputtering of impurity gas atoms from surface

3. Sputtering of loosely bonded solid atoms from surface
4. Solid atoms or ions depositing on surface.
5. Gas atoms contaminating surface.

Cuomo *et al.,* 1991 described the formation of DLC films by non-equilibrium process that involves ion bombardment or condensation of energetic species on the substrate, resulting in metastable phase. The ion bombardment also gives rise to highly dense films resulting in good vapor and liquid barrier properties. Lifshitz, 1999 and Lifshitz *et al.,* 1990 proposed that sp^3 sites are created by preferential displacement of sp^2 sites and the growth of DLC started from subsurface, thus termed it as low energy subsurface implantation. As per Robertson, 1993 subplantation results in an increase in the density and causes local bonding to change to sp^3. Carbon ions lose their energy due to collision with target atoms. The energy at which the ion can pass through the interstice and surface is called the penetration threshold E_p. Displacement threshold, E_d, is the minimum energy needed by the incident ion to displace an atom and create vacancy. E_b is the surface binding energy acting as barrier, then the net penetration threshold for free ions is given by

$$E_p \sim E_d - E_b \quad \text{.....(2.1)}$$

When an ion does not have sufficient energy to penetrate the surface, it sticks to the surface and remains at low energy state of sp^2. When the ion energy is greater than E_p, it penetrates into the subsurface and increases the density. During the film growth, if there is high energy ion bombardment, the densities of carbon films are high, resulting in sp^3 hybridization. On contrary, if there is no energetic ion bombardment, the densities of carbon films are low, resulting in sp^2 hybridization. The entire process is divided into three stages namely (a) collision stage, (b) thermalisation stage and (c) relaxation stage.

In an incident beam of flux *f* and a fraction ϕ of energetic ions with energy E_p, the fraction of ion below the surface is given by

$n = f\emptyset - \beta n$……(2.2)

and this gives $n = \frac{f\emptyset}{1+\beta}$……(2.3)

where n is the fraction of sub-planted atoms in the film

1 – n is the fraction of atoms left on surface as sp^2 sites

β is the constant.

The increase in the density by sub plantation is given by

$\frac{\Delta\rho}{\rho} = \frac{n}{1-n}$……(2.4)

Substituting the value of n, then we have

$\frac{\Delta\rho}{\rho} = \frac{f\emptyset}{1-f\emptyset+\beta}$……(2.5)

where ρ is the density of sp^2 carbon, Δρ is the increase in density

Ziegler *et al.,* 1985 explained the probability of penetration of ions in terms of energy to be

$f = 1 - \exp\left(\frac{-(E-Ep)}{Es}\right)$……(2.6)

E_p is the penetration threshold and E_s is a constant.

They also proposed that penetration could occur either directly or indirectly by knock-on and, in the case of ion beam deposition, it is only knock-on.

With a relaxation rate of $\beta \sim 0.016(\frac{Ei}{Eo})^{5/3}$ and thermal spike of ~10^{12} s, the sub- plantation density becomes

$$\frac{\Delta\rho}{\rho} = \frac{f\emptyset}{(1-f\emptyset+0.016(\frac{Ei}{Eo})^{5/3})} \quad \text{.....(2.7)}$$

where E_o is the diffusion activation energy.

The schematic of sub-plantation by direct penetration, knock-on and relaxation is shown in Figure 2.9

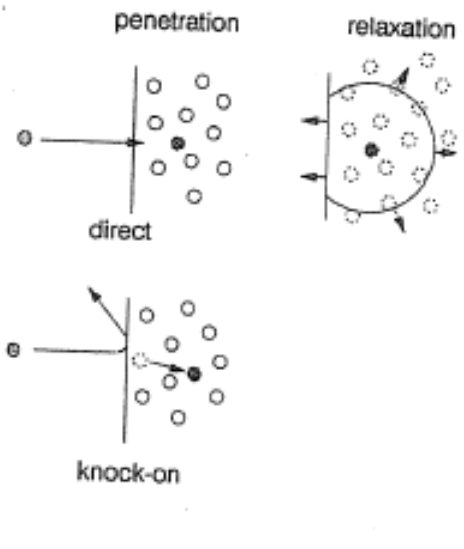

Figure 2.9. Penetration, relaxation and knock-on (Robertson, 2002)

The gridded Kaufman type ion source provides the most independent control of the process parameters. The filament cathode is heated up by a voltage to emit thermionic electrons. When a voltage is applied between a filament cathode and anode ("discharge voltage") the electrons accelerate toward the positive anode, ionize the gas, and initiate plasma. The emitted electrons are usually magnetically confined to increase plasma density, and thus the ion-beam current. A

positive beam voltage is applied to the anode and negative voltage to the accelerator grid to extract positive ions from plasma and form a beam. This beam is neutralized by thermal emitted electrons from a hot filament to eliminate any charge build-up on the substrates. The applied discharge voltage and the gas flow rate into the ion source control the ion species in the plasma, and the beam voltage controls the ion energy impacting the deposition surface.

The ion beams for depositing DLC are generated from methane (CH_4) or other hydrocarbon gases. The gases pass through the ion source and were ionized, and the positive ions are extracted as shown in Figure 2.10. The positive ions extracted from CH_4 plasma form an ion beam and are directed onto the substrate to form a DLC coating and the deposition rate is controlled by the ion-beam current density.

The ion-beam energy is the key parameter in determining the DLC properties and a relationship between hardness, compressive stress and ion-beam energy is shown in Figure 2.11 for a methane source gas. Maximum hardness of 20 GPa is achieved at beam energy in the range of 100 ~ 250 eV, which correlates with maximum compressive stresses. Increasing beam energy results in reduced hydrogen concentration, and thus reduced electrical resistivity, and increased refractive index and absorption coefficient. DLC formed at lower beam energies are usually less dense, softer and more transparent.

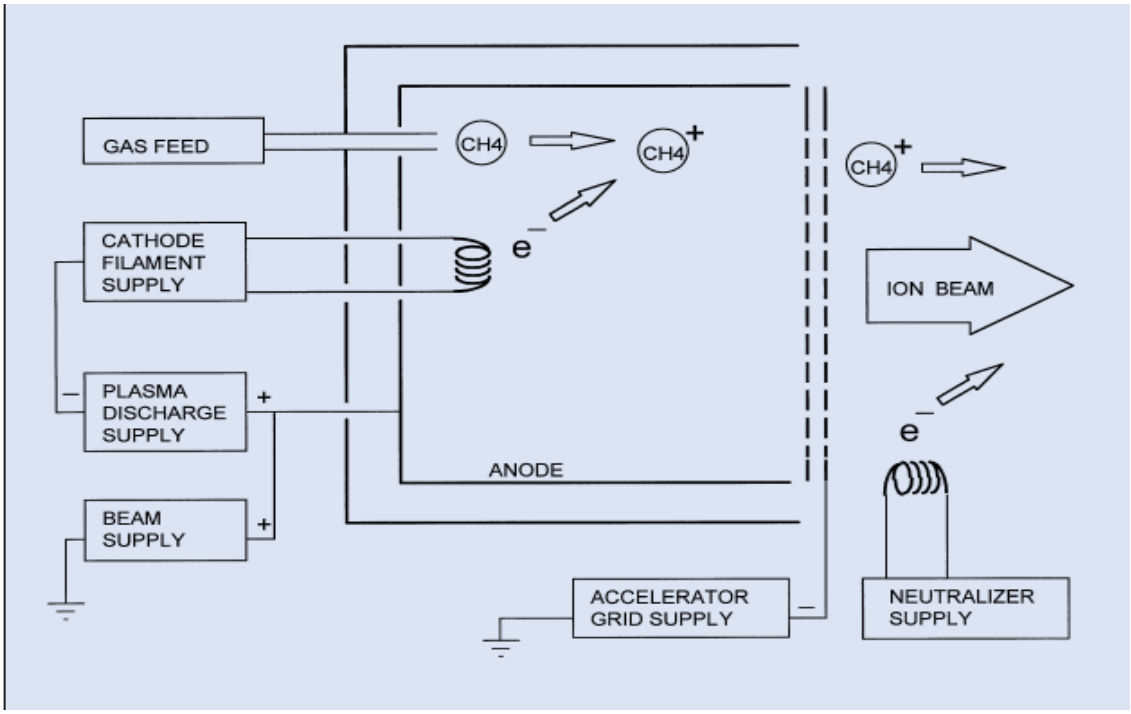

Figure 2.10. Kaufman type gridded ion source (Kimock *et al*)

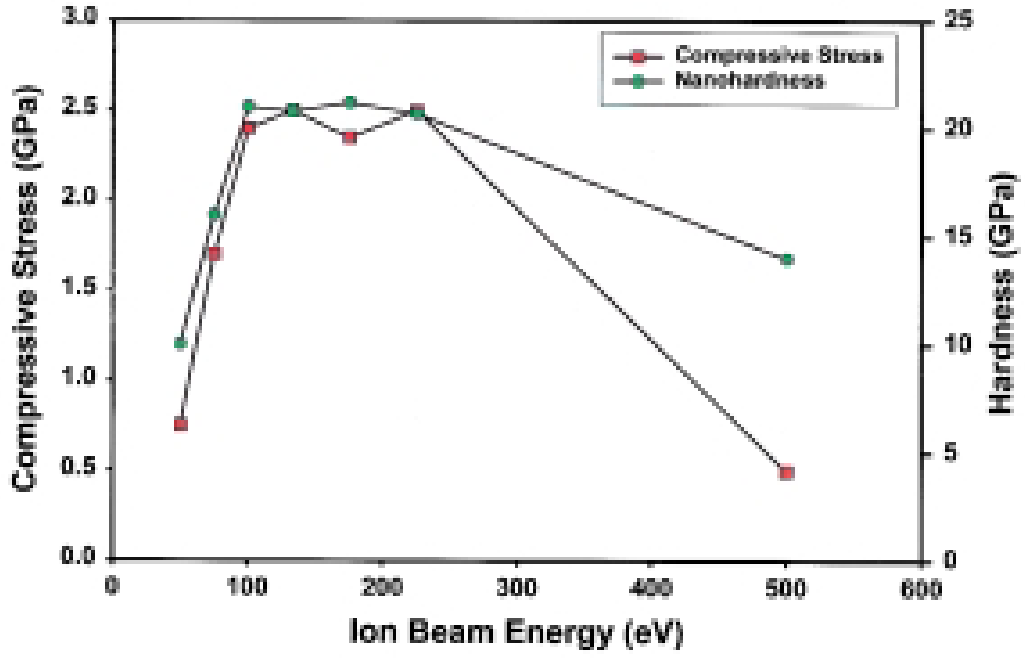

Figure 2.11. Ion beam energy and compressive stresses (Kimock *et al*)

2.1.5 Diamond-like carbon thin films on Polytetrafluroethylene

PTFE is a synthetic fluropolymer obtained as a result of polymerization of tetrafluroethylene molecules and its chemical formula is

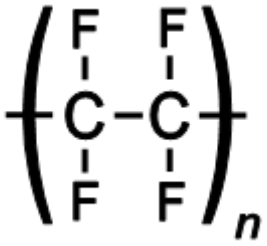

It has a complete outer shell and becomes one of the most inert and stable materials due to its strong carbon-fluorine covalent bonds. The main chain of the polymer is twisted and becomes tightly wrapped by fluorine atoms (Figure 2.12).

Polymers possess many desirable properties for biomedical applications, including a density comparable to human tissues, good fracture toughness, resistance to corrosion, and ease of forming by molding or machining and are increasingly chosen as a material in a variety of implants for widespread applications. However, polymers do not possess good heamocompatibility and often result in thrombus formation when in contact with blood. In order to resolve the problems, diamond like carbon coatings on PTFE has been investigated.

Zheng *et al., 2005* showed that DLC and C-N films deposited by ion beam assisted deposition (IBAD) possessed better heamocompatibility compared to bio metallic materials like NiTi and

316L, and that platelet adhesion increased by increasing surface roughness and was affected by surface energy.

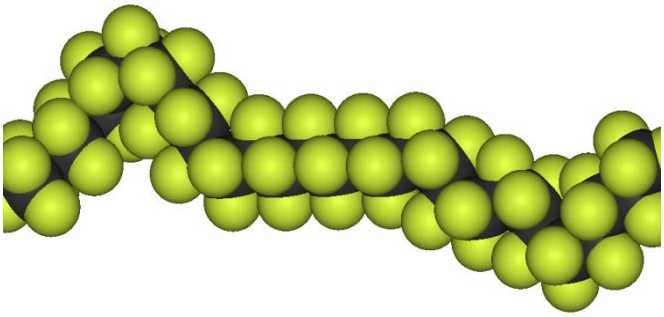

Figure 2.12. PTFE molecules (Foursa, 2007)

Huang yan, 2008 reported less number of platelets adhering to PIID (Plasma Immersion and Ion Deposition) synthesized DLC surface compared to Ti bio material. The results were attributed to the rough surface of Ti materials. However, the platelets on DLC were aggregated.

Hasebe *et al.*, 2006 proved that surface roughness of DLC films did not show any effect on platelet adhesion and activation. Other factors such as wettability, free energy and chemical characteristics of the surface played a major role in determining the platelet adhesion. They reported that the DLC films deposited by plasma enhanced chemical vapor deposition did not show any significant change in platelet adhesion and activation, for roughness ranging from 2nm to 100nm. However, fluorine in DLC inhibited platelet adhesion and activation.

Roy, 2008 investigated the effect of O_2 and N_2 plasma treatment on platelet adhesion and reported hydrophilic DLC surface exhibited improved haemocompatibility by inhibiting fibrinogen and platelet adhesion.

Up to now, there is no relevant research done to explore the heamocompatibility of ion beam synthesized DLC or doped DLC on PTFE. In this research, commercially available PTFE of 0.05mm thick in the form of thin sheet was used as substrate for DLC coating.

2.2 Structural characterization of diamond-like carbon thin films

2.2.1 Raman spectroscopy

Raman spectroscopy is a powerful technique for distinguishing different C-C bonds in diamond, graphite, carbon nanotubes, fullerenes, amorphous carbon and DLC. It has been widely used to analyze the bonding structure of carbon materials. The technique is based on Raman Effect: inelastic scattering or Raman scattering of monochromatic light from a laser source. Light may be in the visible, near infrared or ultraviolet range and interact with phonons (quantized mode of vibration in a rigid crystal lattice) resulting in a shift of energy. Raman shifted photons of light can be either of higher or lower energy depending on vibrational state of molecules and gives information about the modes of phonons in the system. Raman energy levels are shown in Figure 2.13. The sample is illuminated by a laser beam and the light from the illumination is collected by lens and transmitted through a monochromator and collected by a detector.

Raman spectra of different carbon structures are shown in Figure 2.14. Diamond has a single Raman active mode at 1332cm^{-1} that corresponds to the Brillouin zone center and created from the stretching vibrations of C-C pair. Graphite single crystal has an active Raman band at 1580cm^{-1} and is termed “G”, originating from the inter plane vibrations.

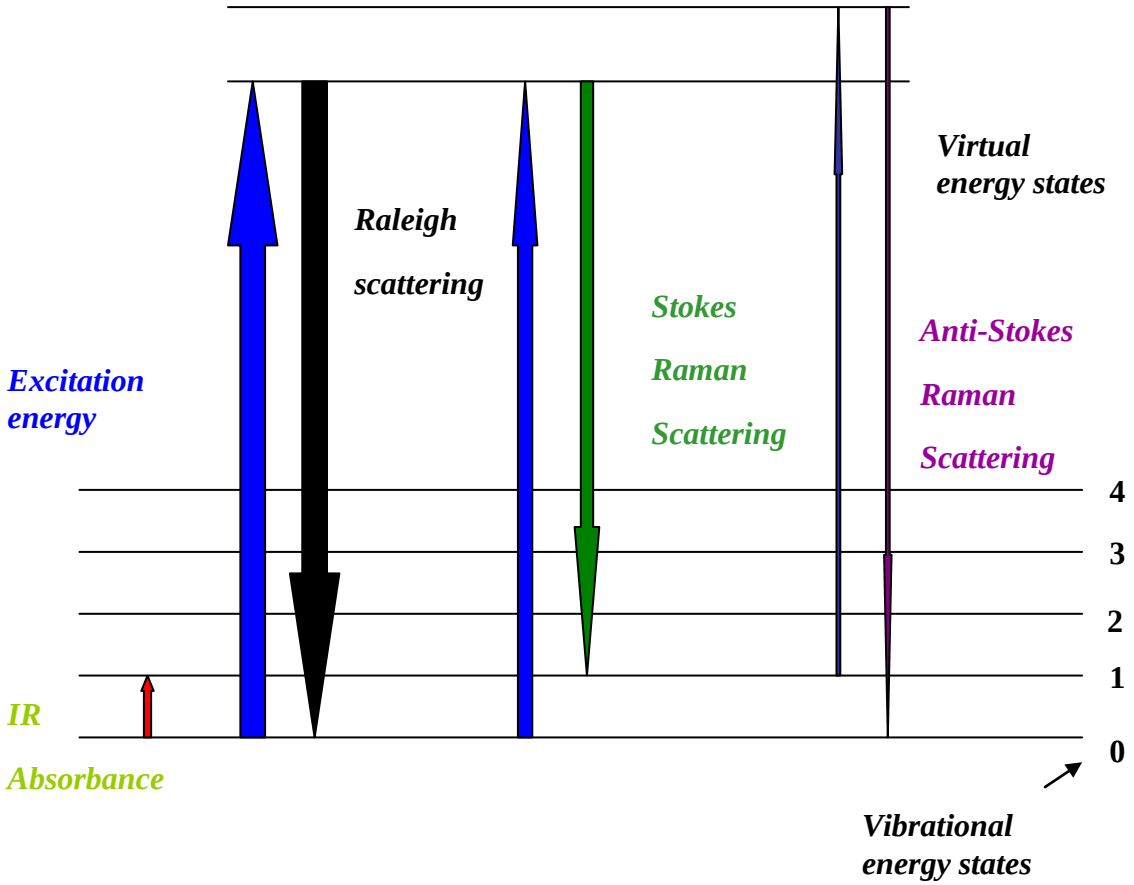

Figure 2.13. Raman energy levels

Disordered graphite has a second mode labeled "D" at 1350cm^{-1} and it corresponds to the breathing vibrations at graphitic cluster boundary. These G and D peaks dominate Raman spectra of most carbon materials even when they contain doping elements as hydrogen and nitrogen (Abrasonis *et al.*, 2006).

Raman spectra of CNx films in the region of 900 – 2000 cm^{-1} exhibit two main peaks at 1350 and 1560 – 1590cm^{-1}, denoted as D and G peaks respectively. G peak is due to the in-plane bond stretching vibrations and can be present either in aromatic clusters or in chain structures (Irmer *et al.*, 2005).

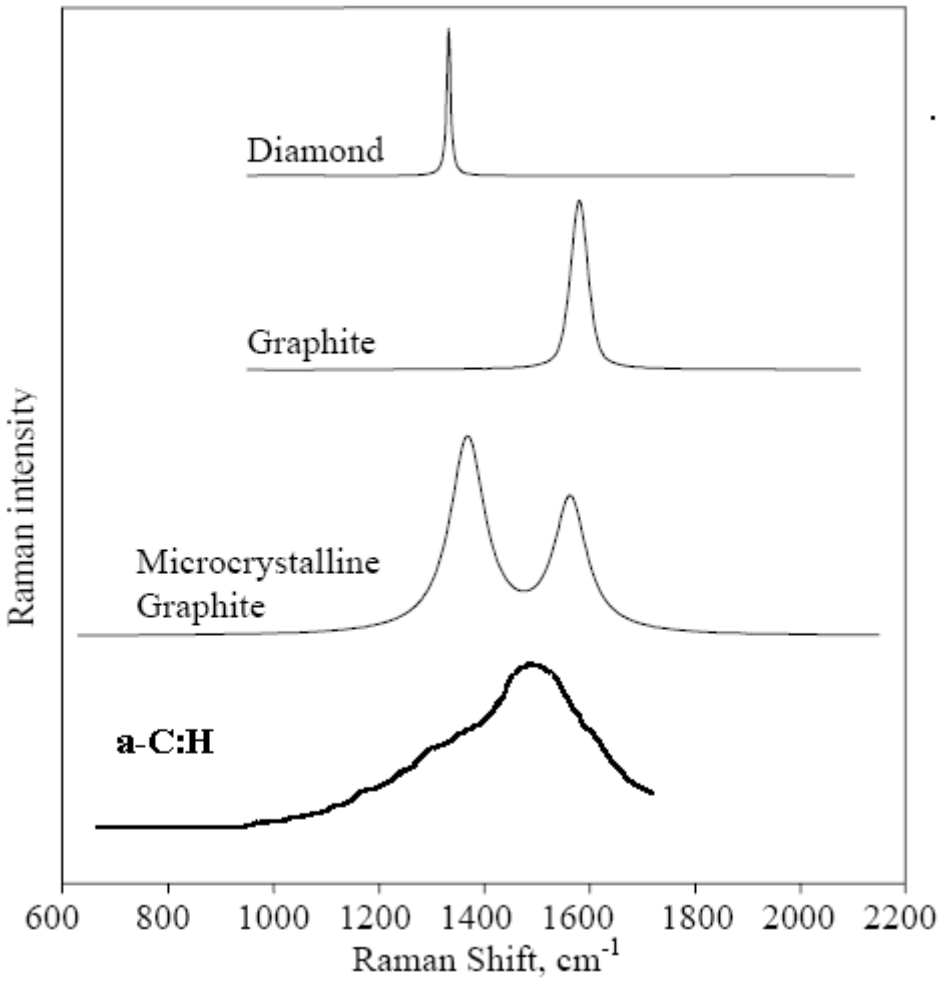

Figure 2.14. Raman spectra of carbon materials (Robertson, 2002)

The disorder peak D is related to the breathing vibrations of aromatic rings. The D peak intensity is sensitive to the cluster size and it decreases as the cluster size decreases with respect to that of G peak (Debdulal Roy *et al.,* 2004). They can be only present in ring structures and hence not seen in complete amorphous C films. Due to the amorphous structure, both D and G peaks for DLC thin films are very broad and overlapped each other. Thus the Raman spectra of DLC are usually fitted with a symmetric Lorentzian D peak and an asymmetric Breit-Wigner-Fano (BWF) G peak. Ferrari, 2000 classified the Raman spectra of all disordered carbons in a three-stage model. Stage 1 is where aromatic rings are maintained with progressive reduction in grain size of ordered graphite layers. Stage 2 corresponds to pure sp^2 network, disordering of graphite layer

and results in loss of aromatic bonding. Stage 3 is where sp^3 increases towards 100% with change of sp^2 rings to short chains. If I (D)/I (G) ratio is nearing zero then it corresponds to stage 3. This relationship gives valuable information to quantify the sp^3 fraction in Raman spectrum. However, Wilmer *et al*., 2006 proposed that the incorporation of nitrogen changes the bonding length compared to pure carbon and enhances the ordering process in disordered carbon network. Nitrogen promotes the cross-linking between adjacent planes and stops the cluster formation.

2.2.2 Scanning electron microscopy and Atomic force microscopy

Atomic force microscopy (AFM) and scanning electron microscopy (SEM) are the two most commonly used techniques for surface morphology investigations. When a voltage is applied to a filament in SEM, it results in emission of electrons from the filament at a high vacuum of 10^{-4} to 10^{-6} Torr. Electromagnetic lenses guide the electrons in the electron column to the sample. The interaction of electrons with the sample, ranging from a few nanometers to a micrometer depending on the beam properties and sample types, results in back scattered and emitted secondary electrons. The secondary electrons from the sample surface are detected through scintillator-photomultiplier. The image is formed due to the intensity of secondary electron emission from the sample at each (X,Y) data point during scanning of electron beam across the surface. The large depth of focus in SEM makes it possible to image rough surfaces of samples as well as in two-dimension. The operation of scanning electron microscope is shown in Figure 2.15.

AFM is highly suitable for producing three-dimensional high-resolution surface topography and can be used both on conductors and insulator materials. Sharp tip at the end of flexible

cantilever, usually made of silicon, is scanned across the sample surface with a constant interaction force. The interaction between the tip and sample is monitored by the laser beam reflecting off the back of cantilever and collected by photodiode detector. The operation of atomic force microscope is shown in Figure 2.16.

Contact and tapping mode are the most commonly used AFM modes. In contact mode, the tip makes soft physical contact with the sample as it scans the surface to monitor changes in the cantilever deflection. The constant force of the scanner tracing the tip across the sample causes the cantilever to bend with the changes in topography. In contact mode, the feed back circuit maintains a constant cantilever deflection by the moving scanner to maintain constant signal to photoelectric detector. The image is generated by the scanner's motion.

In contact mode, the force between the tip and the surface is kept constant during scanning and cantilever drags across the surface and can result in surface damage. In tapping mode the cantilever is driven to oscillate up and down by a small piezoelectric element mounted in the AFM tip holder. Tapping mode is gentle enough even for the visualization of smaller single molecules.

Scanning electron microscope provides two-dimensional image of conductive sample and is operated under a vacuum environment whereas AFM provides a true three-dimensional surface profile and the samples viewed by AFM do not require any special treatments. AFM modes can work well in ambient air and can provide higher resolution than SEM.

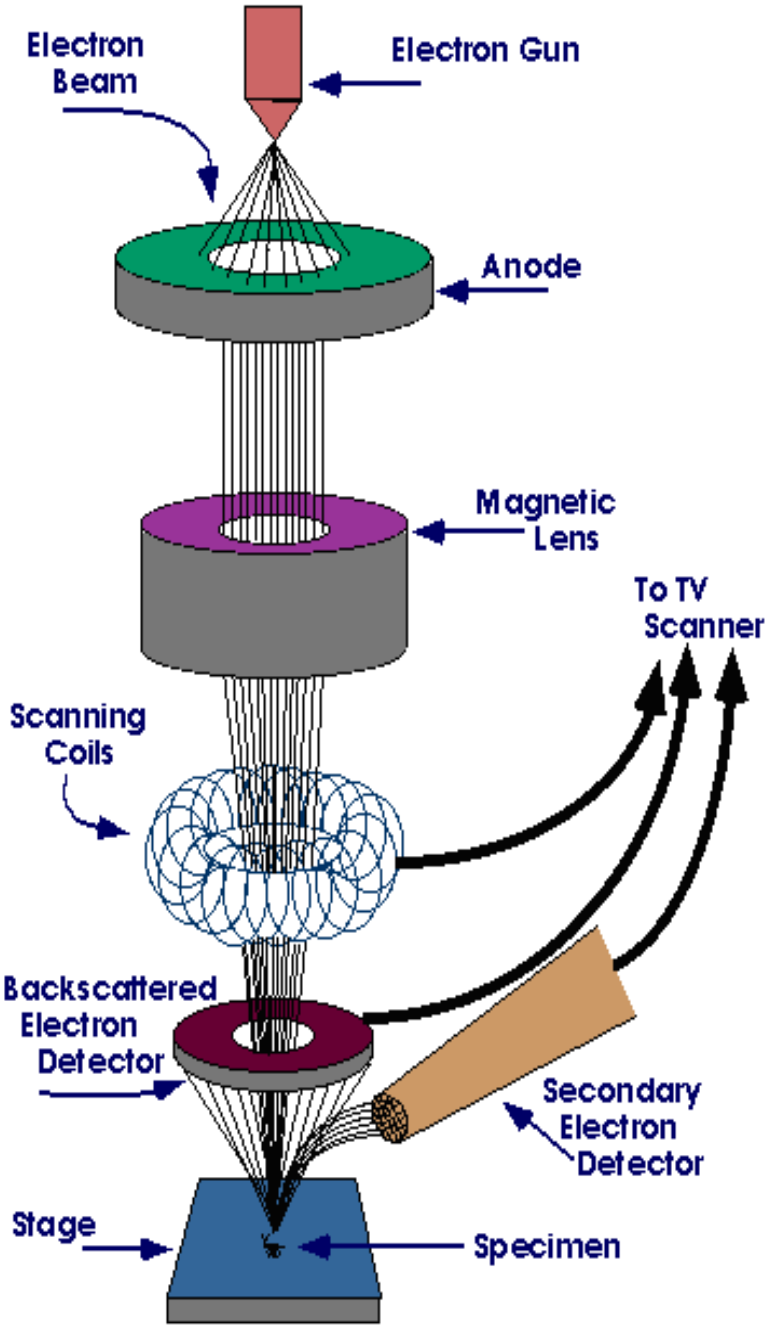

Figure 2.15. Operation of SEM (www.purdue.edu)

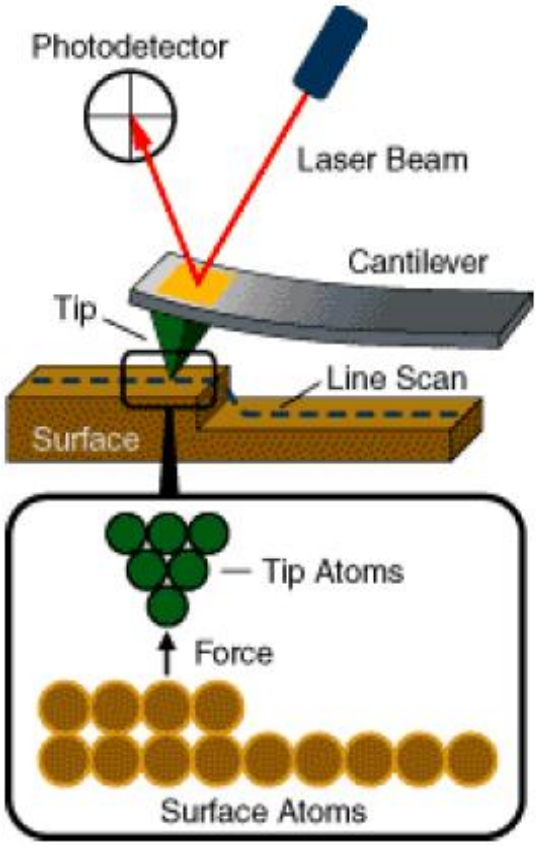

Figure 2.16. Atomic force microscope operation (http://www.Agilent.com)

However, area on the order of millimeters by millimeters with a depth of field on the order of millimeters can be imaged by SEM, whereas AFM can only image a maximum height on the order of micrometers and a maximum scanning area of around 150 by 150 micrometers. SEM can scan in real time while AFM has slow rate of scanning.

2.2.3 X-ray photo emission spectroscopy

X-ray photo emission spectroscopy (XPS) is a technique for measuring elemental composition in the surface based on photo electric effect. The energy of x-ray photons is greater than 1000 eV in

XPS systems. Absorption of such energetic photons leads to removal of an electron from the core or other subshell atomic orbital. The kinetic energy of an escaped free electron is less than the energy of the absorbed photon by some value and is considered the binding energy of the electrons - Einstein's law. The escaping electrons can be analyzed by their kinetic energies and in combination with Einstein's law gives us an idea of elements present in the surface.

Calculated atomic subshell photoionization cross-sections for carbon and nitrogen at different photon energies by Yeh & Lindau, 1985 are given in Figure 2.17. The ionization of 1s orbitals of carbon and nitrogen requires 285 eV and 400 eV with an incident photon energy of 1000 eV.

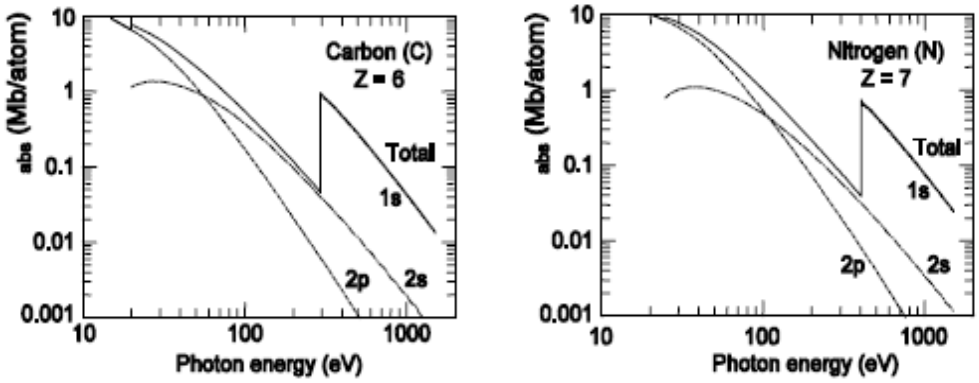

Figure 2.17. Atomic sub shell photoionization cross-sections for carbon and nitrogen (Yeh and Lindau, 1985)

2.3 Property Characterization of Diamond-like Thin Films

2.3.1 Mechanical properties

The mechanical properties of DLC films are of great interest due to its application as protective coatings such as disks and recording heads. Many of the mechanical properties are often measured by nano-indentation. Nano-indentation tester is a high precision instrument for the determination of local mechanical properties of a surface layer. The force-displacement curve was measured when a diamond tip was forced into and unloaded from a surface. The hardness is the pressure under tip and calculated by the ratio of force to the projected area of plastic deformation.

Hardness $H = 0.0378\, L_{max} / h^2_p$ .....(2.8)

where L_{max} is the maximum load

h_p is the plastic deformation and is the intercept drawn by a tangent to the unloading curve as shown in Figure 2.18.

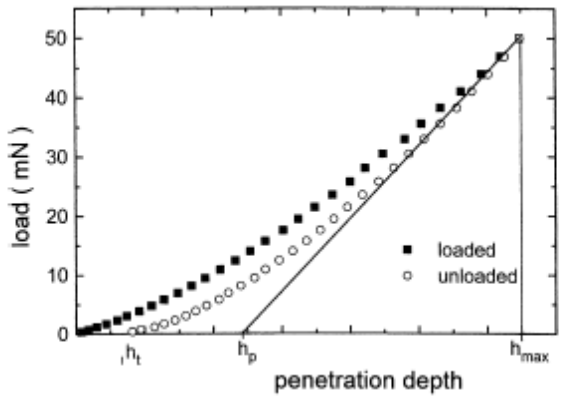

Figure 2.18. Loading – unloading curve of nanoindentation

and the Young's modulus is given by Equation 2.9.

$$E = 0.179 \frac{(1-\nu^2)L_{max}}{(h_{max}-h_p)h_p} \quad \text{.....(2.9)}$$

where ($h_{max} - h_p$) is the elastic deformation (length from the intercept h_p to the maximum indent h_{max} , v is the poisson ratio.

Hardness is related to the yield stress Y and Young's Modulus E by the relationship

$$\frac{H}{Y} = 0.07 + 0.06\ln\left(\frac{E}{Y}\right)$$ (Robertson, 2002)……(2.10)

H/Y ~1.8 for a material like diamond with a low Y/E ratio

In this study, mechanical properties (hardness and Young's modulus) of DLC films coated on Si substrates were measured by Berkovich nanoindenter manufactured by the Centre for Tribology Inc.

There are numerous techniques known for adhesion and delamination testing, some of the most common being a tape test, stud-pull test, scratch test and an indentation test. Scratch test is the most widely used techniques for hard coatings. In the scratch test, where an indenter moves in both vertical (loading) and horizontal (sliding) directions, and an acoustic emission sensor allows for detection of the initiation of fracture, while the scratch pattern indicates the type of failure.

2.3.2 Wettability and contact angle

The surface energy of a material is a parameter that determines the adsorption, wetting and adhesion properties of the material. It is usually characterized by contact angle measurements. When the surface energy is low, the contact angle is high. A surface is said to be hydrophobic when the contact angle is above 90°.

The effect of surface roughness on wettability and contact angle has been the subject of numerous studies. In order to evaluate the wettability and contact angle of DLC films, PTFE substrates with and without DLC coating were quantified by measuring the static water contact angle. The contact angles were measured from a profile of liquid distilled water drops placed on the PTFE substrates at room temperature. The values of the water contact angle are average from 2 samples. Static contact angles were measured with a microscope equipped with CCD-video, prism and stand with tiltable plane. Pictures taken by this method were analyzed using image processing program. The accuracy of the contact angle measurements were 1°. The contact angles for DLC in previous studies reported by Mirjami Kiuru and Esa Alakoski, 2004 are typically 70° - 80°.

Surface energy can be calculated by using Young – Dupre equation

$$E = \gamma (1+\cos \theta) \quad \text{.....(2.11)}$$

where γ is the surface tension of water at 20 °C (γ = 72.8 mN/m) and θ is the contact angle (°)

2.3.3 Haemocompatibility

When a material is implanted into the body, it is the surface of the material that comes into contact with blood and living body. If the implanted material surface stimulates a too strong biological response, the implanted material will not be able to perform its function. If the adhesion of cells and tissues to the implanted device surface is too poor, infections may be created due to the empty space in between them (Ikada, 1994). Therefore, the implants' surface should show the least foreign-body reactions and secondly cell and tissue bonding capability. However, many materials do not have such surface properties. The purpose of surface modification is to improve the surface properties of materials to improve their biocompatibility.

Interaction of blood with foreign material can result in blood coagulation (thrombosis) and blood tissue damage (cell death and release of contents – hemolysis). Thrombus formation includes interaction between blood proteins, cells and artificial material surface (Courtney *et al.*, 1994). The rapid adsorption of proteins onto material surface is the first major reaction induced by blood-material interaction. The absorption and adhesion of proteins and platelets greatly affect the thrombogenicity of artificial surfaces. Features like platelet activation, intrinsic, extrinsic coagulation, control systems participating in thrombus inhibition and fibrinolysis contribute to blood coagulation. Another important feature of blood – material interaction is that blood contact with material surface generally induces adhesion and aggregation of platelets. Human blood cells consist of platelets called thrombocytes along with red blood cells (erythrocytes) and white blood cells (leukocytes) as shown in Figure 2.19.

The adsorbed protein layer is a controlling factor of platelet response and the platelet adhesion is followed by platelet release reaction and platelet aggregation on the surface. Platelet adhesion, aggregation and activation with thrombin release are the sequential steps involved in thrombus formation (Vasilets *et al.*, 2005). A possible way to improve haemocompatibility is to enhance albumin adsorption. Several research works are being carried out in this area.

The blood compatibility, haemocompatibility, includes the analysis of proteins and platelets in contact with blood. Quantification of amount of platelets adhered to surface can be done by radiolabelling (Cui *et al.*, 2000).

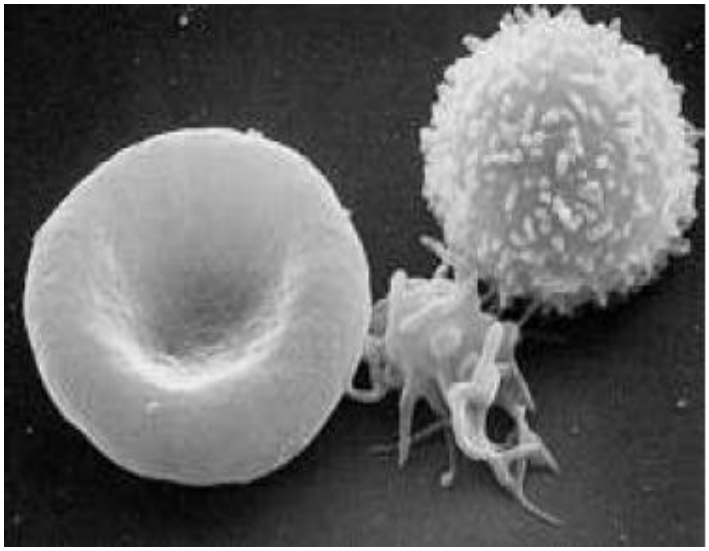

Figure 2.19. Human blood cells (From left Erythrocyte, thrombocytes and leukocyte) (http://en.wikipedia.org)

Scanning electron microscopy provides information about total amount as well as the degree of aggregation and activation of platelets. Thrombus formation is complicated and a series of reactions including precipitation of proteins (fibrinogen, albumin etc), cells (red blood cells, white blood cells and platelets) from blood occurs (Tirrell *et al.*, 2002).

In a recent study by Zheng *et al.*, 2005, it is found that the blood clotting time decreases as the surface roughness of the DLC coatings increases. An increase in nitrogen concentration of the film has resulted in decrease in the platelet adhesion.

PTFE and other fluorocarbon polymers are strongly hydrophobic and result in a net attraction of hydrophobic proteins. Hydrophobicity is to be reduced by means of surface modification. Surface roughness is also critical to minimize the cell adhesion on blood contacting biomaterial surface for enhanced haemocompatibility (Black, 1999)

CHAPTER 3

EXPERIMENTAL METHODS

3.1 Ion Beam Deposition of Diamond-like Carbon Thin Films

DLC thin films were synthesized by ion beam deposition. This deposition system was manufactured by 4wave and its schematic view is shown in Figure 3.1. It consists of a high vacuum chamber, a high vacuum pumping system with a turbo and a mechanical pump, a Kaufman ion source with a tungsten filament neutralizer for direct ion beam deposition, a rotating substrate holder that can be inclined from 0° to 90°, a constant water cooled stage, a 6-target assemble, and a sputtering ion source. The deposition system can be used for deposition of DLC thin films either by ion beam deposition or by ion beam assisted sputtering deposition. Ion beam assisted sputtering deposition uses sputtered graphite as carbon source, thus hydrogen free DLC (a-C) thin films are deposited, whereas direct ion beam deposition uses methane as carbon source, thus hydrogenated DLC (a-C:H) thin films are deposited.

The essential features of the direct ion beam deposition are

1. Source of ion deposition with energies in range of 40 eV to hundreds of eV.
2. High vacuum region between ion source and substrate to reduce charge exchange and energy loss due to collisions between ion beam and background gases.
3. Substrate in a high vacuum region in vicinity of ion beam.

4. Heat sink to eliminate excess energy from surface of substrate.
5. Thermionic filament or hollow cathode, to neutralize the ion beam and avoid net charge building up, by injecting electrons.

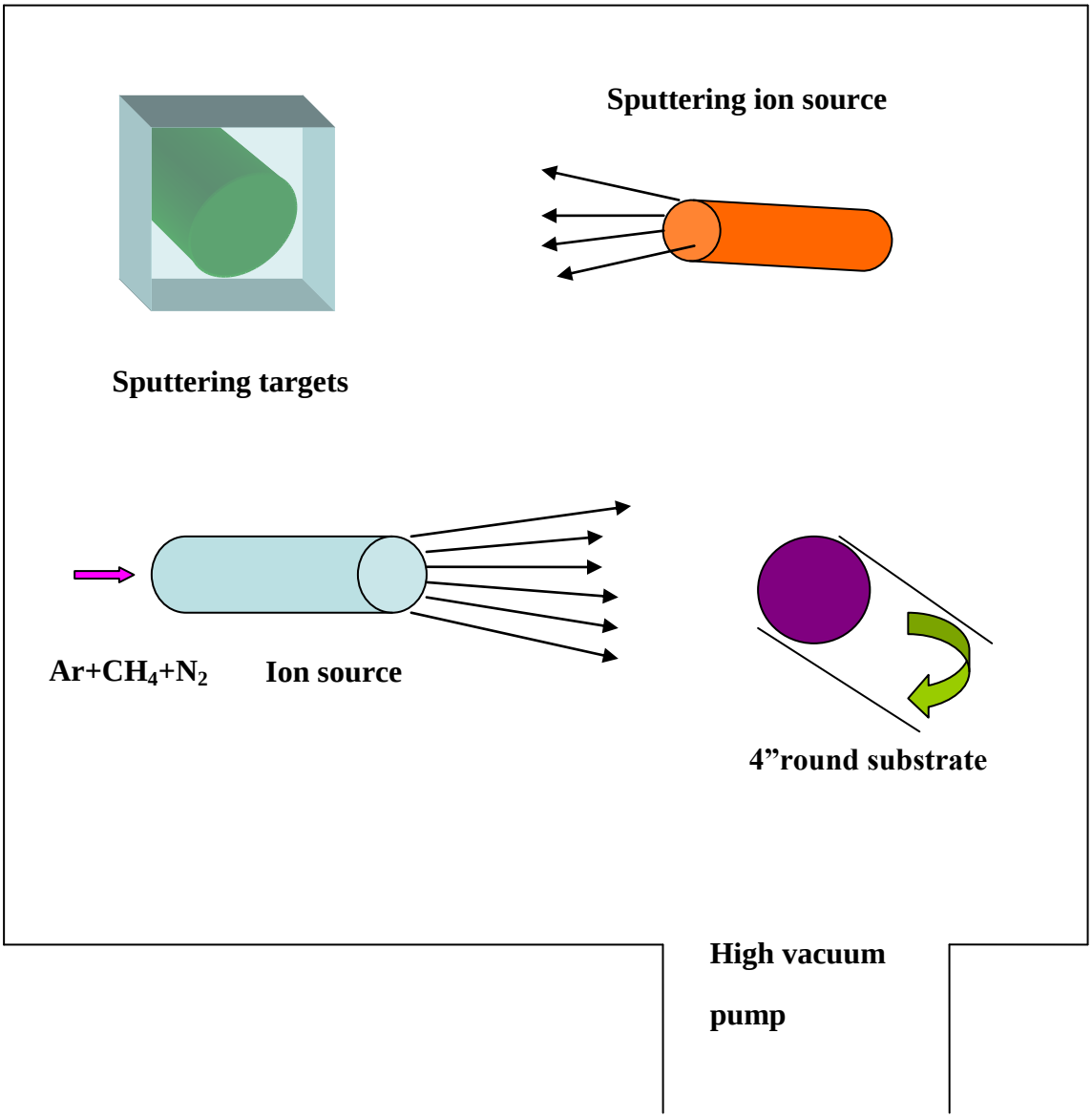

Figure 3.1. Ion-beam deposition system

In this thesis, only ion beam deposition technique was used to deposit DLC thin films. The DLC thin films were synthesized with energies of 250 eV and 300 eV and a beam current of 75 mA. Prior to commencing the deposition, the substrates (PTFE sheets and Si wafers of 0.1 mm and

0.5 mm thickness, respectively) were Ar^+ ion sputter cleaned with beam energy of 800 eV for 15 minutes. During the DLC deposition, high purity methane and argon were ionized simultaneously in the ion source and directed toward the substrate, whereas nitrogen delivered directly into the deposition chamber for synthesizing NDLC thin films. N_2 flow rates equal to 0, 2 and 5 SCCM of the gas flow rate were used and the corresponding samples were identified by DLC, NDLC and 5-NDLC. All the films were deposited for a time period of 4 hours to ensure sufficient thin film thickness for investigations of structures and properties including haemocompatibility. The deposition parameters followed for DLC synthesis on Si and PTFE substrates are shown in Tables 3.1 and 3.2 respectively.

Table 3.1. Deposition parameters on Si (100)

Parameters	**Si (100) Wafer 1**	**Si (100) Wafer 2**	**Si (100) Wafer 3**	**Si (100) Wafer 4**
Base Pressure (Pa)	4.85 E- 07	5.0 E- 07	4.30 E- 07	4.0 E- 07
Working Pressure (Pa)	7.08 E- 04	5.39 E- 04	5.0 E- 04	5.35 E- 04
Ion Energy (eV)	300	250	250	300
Ion Current (mA)	75	75	75	75
Total gas (sccm) ($Ar+CH_4+N_2$)	32	32	34	34
Argon	24	24	24	24
Methane	8	8	8	8
Nitrogen	0	0	2	2
Deposition time (h)	4	4	4	4
Deposition temperature °C	25	25	25	25
Coating thickness (nm)	550	550	500	500

Table 3.2. Deposition parameters on PTFE

Parameters	**PTFE 1**	**PTFE 2**
Base Pressure (Pa)	2.80 E- 06	2.00 E- 06
Working Pressure (Pa)	7.08 E- 04	7.08 E- 04
Ion Energy (eV)	250	250
Ion Current (mA)	75	75
Total gas (sccm) ($Ar+CH_4+N_2$)	32	34
Argon	24	24
Methane	8	8
Nitrogen	0	2
Deposition time (h)	4	4
Deposition temperature °C	25	25

3.2 Structural Characterization

Raman spectra were measured on samples using a Renishaw system (model 2000) operated at 514 nm Ar ion laser with a spot size of approximately 2 μm at the Saskatchewan Structural Science Centre. A picture of the Raman spectroscope is shown in Figure 3.2. Si and PTFE samples 1cm x 1cm square were placed underneath the microscope and three spots were chosen to obtain Raman spectra for each sample.

Hitachi S-3000N variable pressure SEM was used to observe the samples surface. It was operated at an accelerating voltage of 15 kV. A picture of the SEM is shown in Figure 3.3.

5 mm round discs were cut from PTFE substrates and were gold sputtered to make them conductive before examination under SEM.

Figure 3.2. Raman Spectroscope - Renishaw model 2000

Figure 3.3. Scanning Electron Microscope – Hitachi S3000N

Surface roughness measurements were done using a contact mode Atomic Force Microscopy (AFM) at the Saskatchewan Structural Science Center (SSSC), University of Saskatchewan. Typical AFM equipment is shown in Figure 3.4.

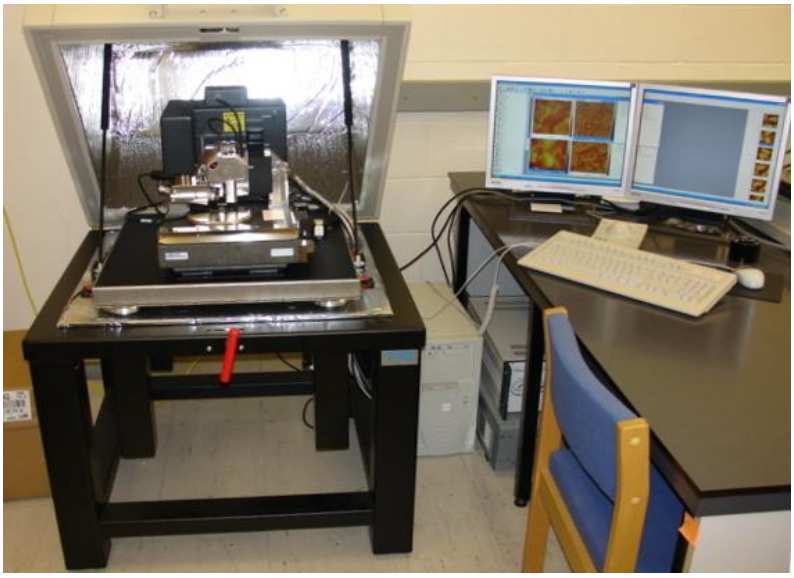

Figure 3.4. Atomic Force Microscopy

3.3 Mechanical Property Characterization

Mechanical properties of DLC films coated on Si substrates were measured by nanoindentation using a Universal Mechanical Tester (UMT) manufactured by Center for Tribology Inc. A Berkovich indenter tip was used for the Nanoindentation Testing. The indenter was normal to the surface and was driven into the sample by applying an increasing load up to a preset value. The load was then gradually decreased until partial or complete relaxation of the sample has occurred. The load and displacement were recorded continuously throughout this process to produce a load-displacement curve from which the nano-mechanical properties such as hardness, Young's modulus, stress-strain relationship, plastic & elastic energy of the sample material were

calculated. The tester applies forces ranging from 0.1 µN to 1 kN, senses depth ranging from 0.1 nm to 100 mm, and uses indenters with sizes ranging from 50 nm Berkovich tips to 12.7 mm balls. Multiple indents on a specific sample area can be obtained automatically with a lateral resolution of 0.5 µm. The UMT tester is shown in Figure 3.5.

Figure 3.5. UMT Nanohardness tester

In this thesis, the Nanoindentation Testing was conducted in three different locations for each sample. For each loading/unloading cycle on each spot, the applied load value was plotted with respect to the corresponding position of the indenter. The resulting load/displacement curves provided data specific to the mechanical nature of the sample under examination. Inbuilt software using established models were used to calculate the quantitative hardness and modulus values for such data. For all samples, the maximum load was 45 mN, loading and unloading speed was 10 mN/min.

The UMT purchased from The Center of Tribology Inc. can perform scratching test to measure the adhesion of the thin films. Specimens in a wide variety of shapes and dimensions can be tested using UMT. Acoustic emission and the sudden changes of electrical resistance and friction coefficient are used to sense the adhesion failure of the thin films. In this work, scratch test was performed in fully computerized UMT with Tungsten carbide blade as scratching object. A load was applied via a closed-loop servo-mechanism and was programmed to increase linearly from 0.1 mN to 1 kN. Friction force (Fx), normal load (Fz), electrical contact resistance (ECR), and contact acoustic emission (AE) were measured and recorded for analysis of critical loads. The sample size was 5cm x 5cm and the testing configuration is shown in Figure 3.6.

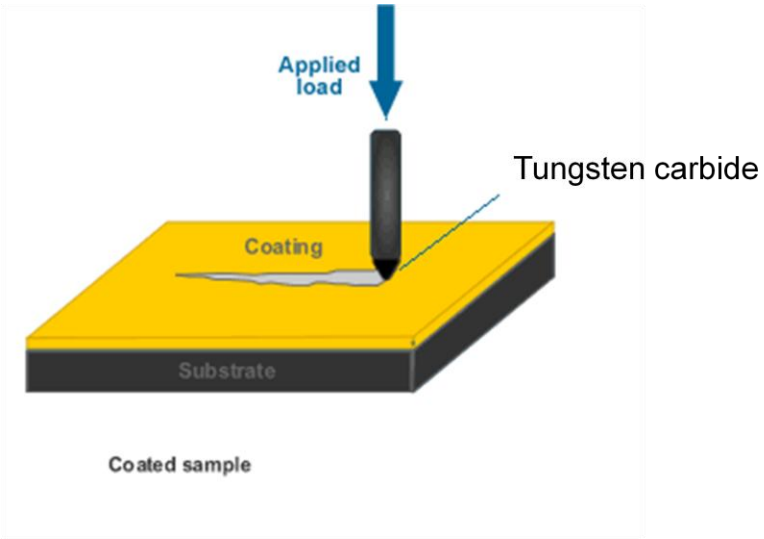

Figure 3.6. Scratch test

3.4 X-ray Photoemission Spectroscopy

XPS measurements were performed at SGM beam line at Canadian Light Source (CLS), University of Saskatchewan, using synchrotron X-ray source simulated to Mg K-α at 1260 eV

photon energy. Peak areas were measured, and divided by the atomic sensitivity factors to calculate elemental composition (Moulder *et al*., 1995). The data was measured and reported by beam line scientist Robert Blyth.

3.5 Haemocompatibility testing

Blood was collected from a healthy donor who was under no medication for at least 10 days prior to the donation and was collected in tubes containing anticoagulants. Small amount of blood was centrifuged in one 50 ml tube, for 15 min at 890 rpm and room temperature. Platelet-rich plasma (PRP) was obtained from upper solution. Small amount of platelets was labelled at room temperature. The suspension was incubated for 2 hours at 37 ºC and rinsed before measuring adhered platelets using fluorescent gamma scintillation counter. Platelet rich plasma from blood and experiments with platelets were done by Dr. Haas from Department of Health Sciences, University of Saskatchewan.

Platelets obtained by centrifugation of human blood were used to study adsorption on 5mm round disks. 50 ml of PRP were placed on the bare PTFE, DLC coated PTFE and nitrogen doped DLC on PTFE for 15 minutes and 60 minutes at room temperature. Platelet activation was studied using SEM.

CHAPTER 4

RESULTS AND DISCUSSION

In this chapter results obtained from Raman Spectroscopy, surface roughness, XPS analysis, nanohardness, critical loads, coefficient of friction and platelet adhesion are presented and discussed. All characterizations were done on DLC and Nitrogen doped DLC. NDLC mentioned hence forth corresponds to doping of nitrogen with 2 sccm N_2 and 5-NDLC corresponds to doping of nitrogen in DLC with 5 sccm N_2.

4.1 Raman Spectra

Raman spectra of film samples deposited on Si and PTFE substrates with different nitrogen doping levels are shown in Figures 4.1 - 4.4. A wide band ranging from 1100 to 1800 cm^{-1}, typically attributed to DLC thin films, appears for all samples. According to Wagner's model developed for Raman scattering of carbon, peaks at 1575 cm^{-1} and 1360 cm^{-1} are assigned to G and D bands, respectively. Both peaks are very broad and are typical for amorphous carbon structures. It has been reported that I_d / I_g, the ratio of integral area under D and G bands are closely related to sp^3/sp^2 ratio in film. The sp^3/ sp^2 ratio is the most important factor in determining the feature of Raman spectra.

I_d / I_g values are 0.58 and 0.61 for DLC and NDLC coatings on Si, respectively, whereas I_d / I_g increases to 0.79 and 0.78 for DLC and NDLC coatings on PTFE sheets, respectively. The

relative Raman peak intensities do not change much with nitrogen doping, suggesting that the carbon substituted by a small amount of nitrogen did not change the vibration modes significantly. However, the I_d / I_g ratio for coatings on PTFE is much higher than those on Si, indicating that the sp^3 concentration in the coatings on PTFE is lower than those on Si. This is also evident from the shift of G band (1553 and 1547 cm^{-1} for coatings on Si against 1582 and 1585 cm^{-1} for coatings on PTFE (Sui and Cai, 2006).

Weaker peaks at about 2200cm^{-1}, corresponding to the carbon-carbon or carbon-nitrogen triple bonds, were also observed.

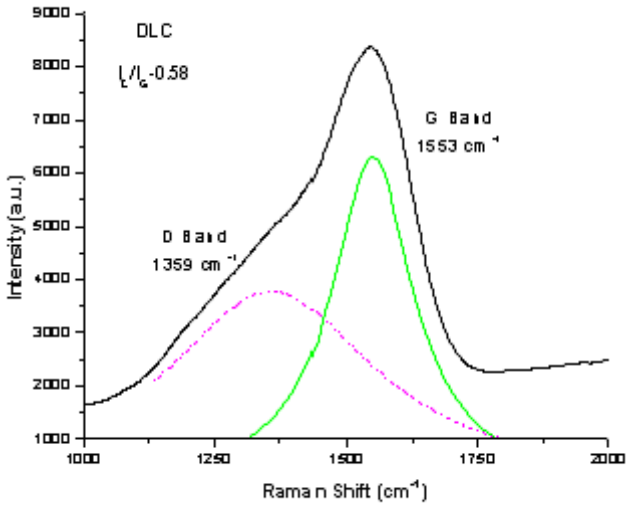

Figure 4.1. Raman spectra of DLC on Si

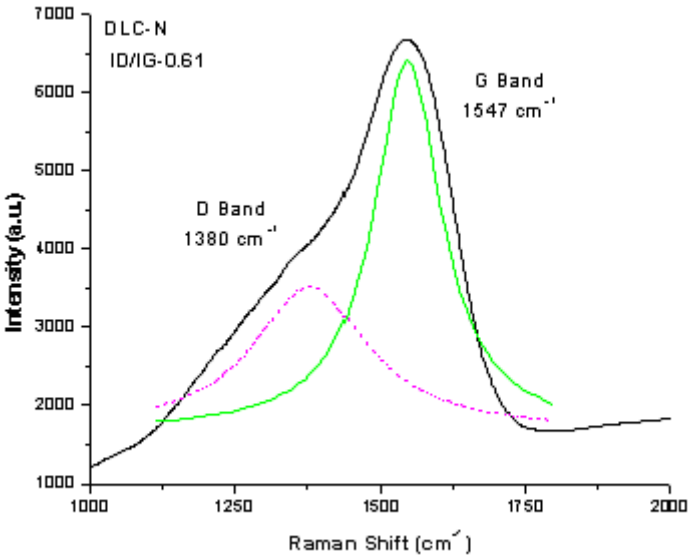

Figure 4.2. Raman spectra of nitrogen-doped DLC on Si

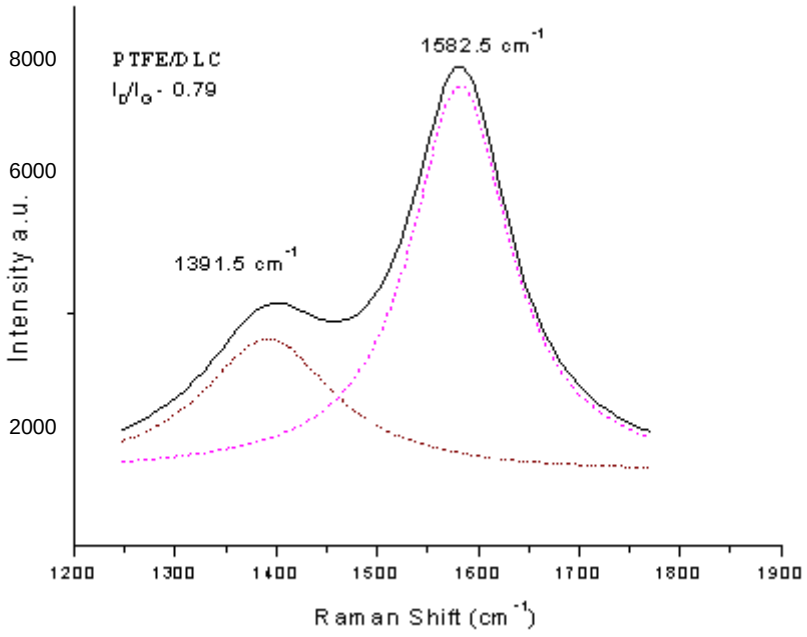

Figure 4.3. Raman spectra of DLC on PTFE

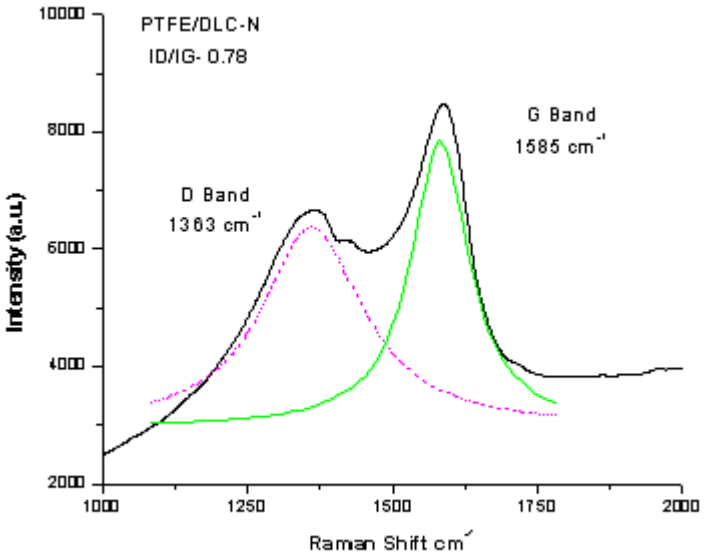

Figure 4.4. Raman spectra of nitrogen-doped DLC on PTFE

4.2 SEM and AFM Observation

The SEM image of the DLC thin films is shown in Figure 4.5. It reveals that the films are dense, smooth, uniform, and amorphous with no pores and discontinuity. None of the special features such as grains were observed in SEM. AFM pictures of virgin, DLC coated and NDLC coated PTFE are shown in Figures 4.6 - 4.8 respectively.

Uncoated virgin PTFE exhibited a complex fibril-like structure with an average surface roughness of about 75 nm. Coating of DLC on PTFE increased the surface roughness to about 197 nm. However, doping with nitrogen makes the surface much smoother and the average roughness was found to be 135 nm. The surface roughness tends to be lower with low nitrogen content in the film as per the results published by Prioli *et al.,* 1996.

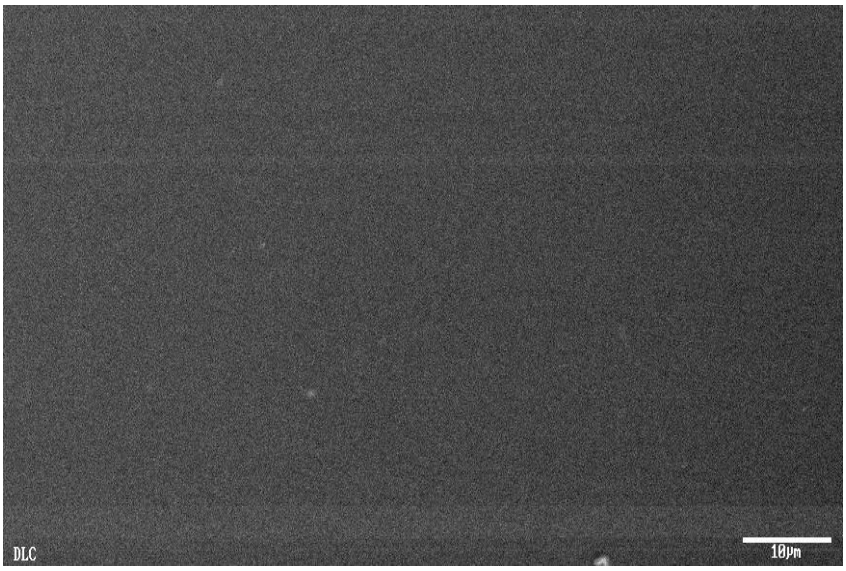

Figure 4.5. SEM image of DLC

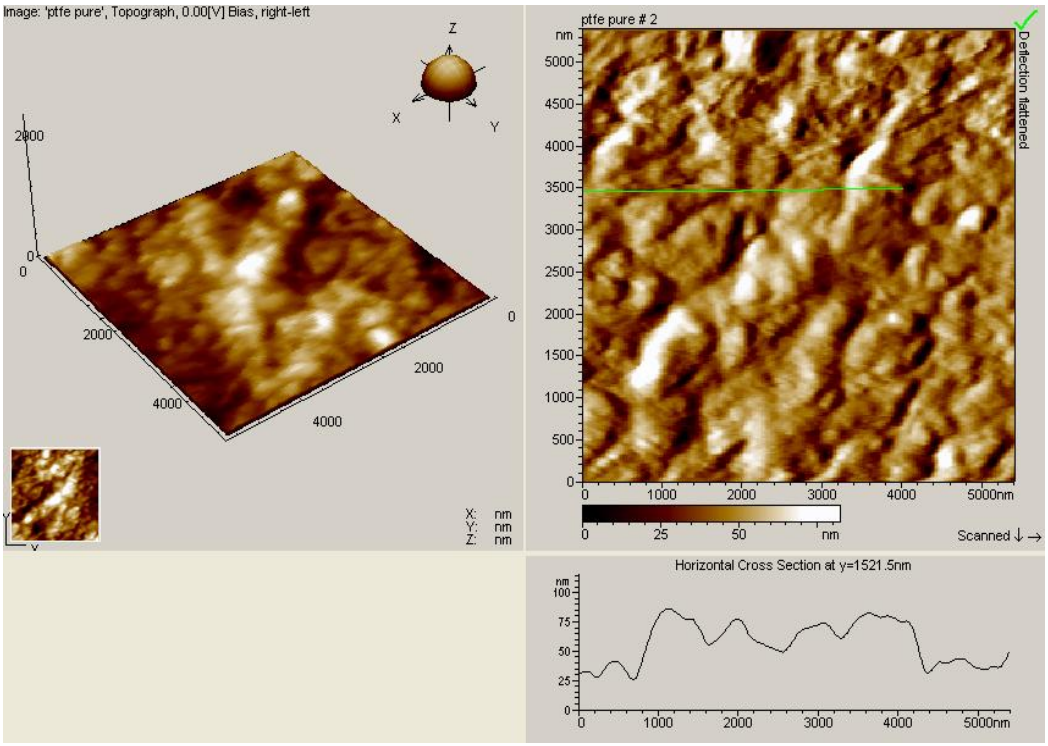

Figure 4.6. AFM image of virgin PTFE

The surface morphology of DLC and NDLC films showed good homogeneity. The DLC film contained fine asperities due to large percentage of sp^3 bonded carbon formed due to the high energy ion bombardment during deposition. The nitrogen doping caused the surface to appear aggregated and this may be due to the clustering of sp^2 sites (Liu *et al.*, 1999). The observation clearly shows that nitrogen doping helps to smoothen the surface.

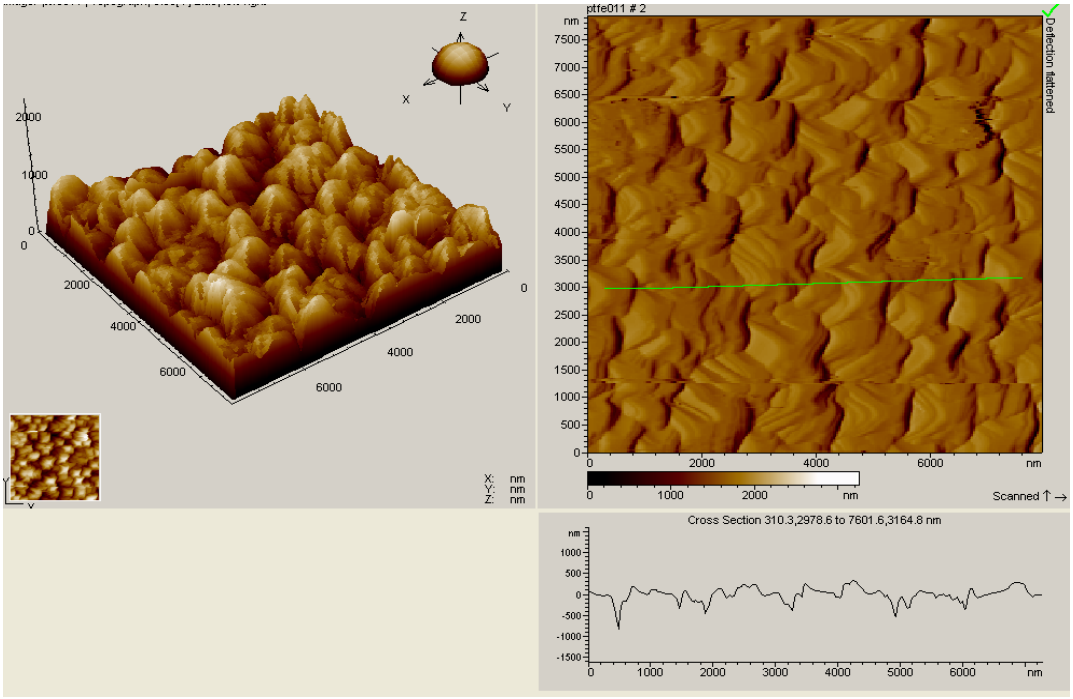

Figure 4.7. AFM image of DLC coated PTFE

The non equilibrium surface atoms have higher average energy than the substrate and this energy corresponds to high free surface energy and that is equivalent to high surface tension. The system tends to reach lowest energy state and according to principal of virtual work, the drive to minimum energy corresponds to drive to minimum area. The surface tension of non equilibrium atoms is unusually large and produces a strong driving force to minimize surface area. This surface area includes the surface irregularities, pinholes and this strong drive to minimize area

helps to produce surfaces with fewer irregularities, less pinholes and makes the film smoother than the substrate.

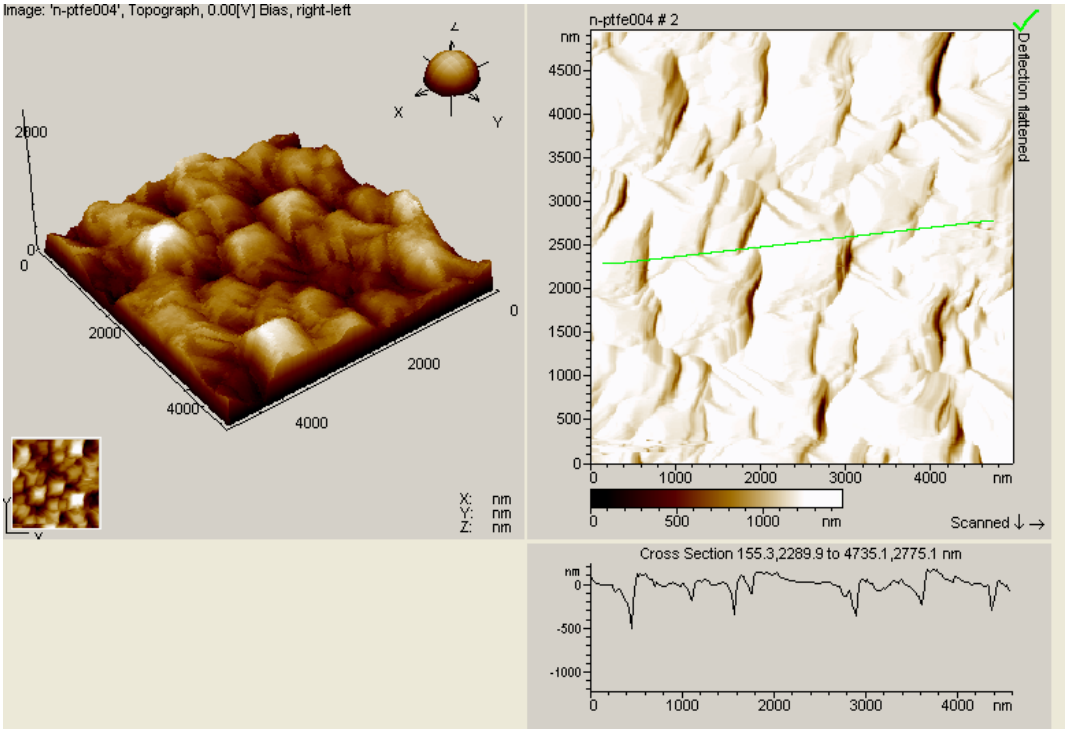

Figure 4.8. AFM image of NDLC coated PTFE

4.3 XPS surface Characterization

XPS was used to determine the chemical composition NDLC on Si. Figure 4.9 shows the XPS spectrum of deposited NDLC. As seen from the spectrum, a small amount of oxygen was observed in the films due to the exposure of the samples in ambient air before XPS measurement. The surface concentrations calculated from the measured integral intensities of the XPS peaks are: 60 at.% C, 10 at.% N and 17 at.% O and are shown in Table 4.1.

The XPS spectrum of C 1s is shown in Figure 4.10, denoting the presence of a large peak at 285.1 eV that corresponds to sp^3 C-C bond on the surface and also sp^2 C=C bond at 284.4 eV. Another peak at 292.7 eV is attributed to π-excitation, which appears in all carbon-based materials having double bonds (Bourgoin *et al.*, 1999, Merel *et al.*, 1998).

The XPS spectrum of N 1s in NDLC (Figure 4.11) shows the presence of two peaks at 398.2 and 400.2 that correspond to the presence of sp^3 CN and sp^2 CN bonds (Junying *et al.*, 2006). The peak of O1s is located at 530.4 eV, which is attributed to C–O bonding (Baba, 2006).

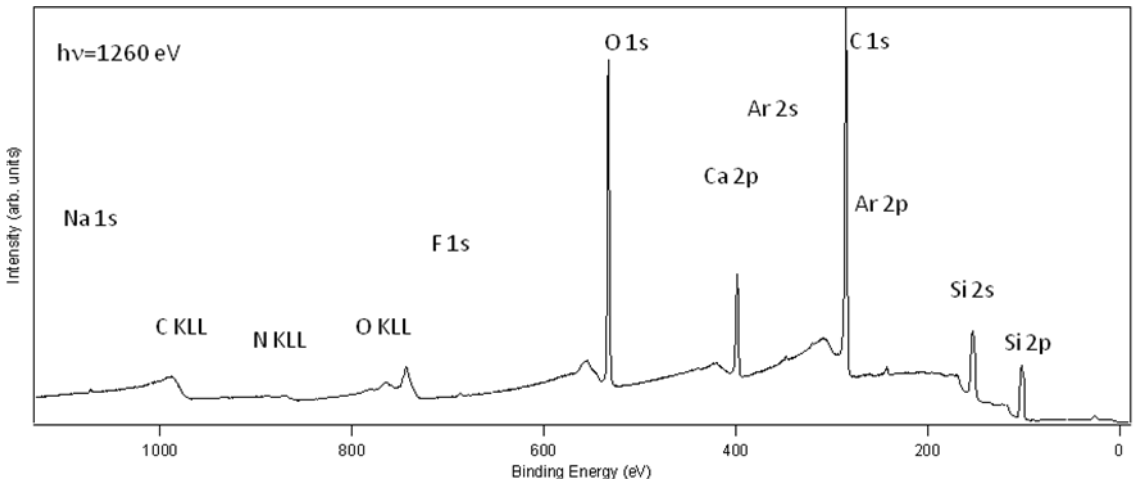

Figure 4.9. XPS spectrum of NDLC film

The XPS spectrum of Si 2p in Figure 4.12 shows the presence of SiO (102.3 eV) and SiO_2 (103.4 eV), which probably due to the contamination. A very weak peak at 99.1 eV was also observed that corresponds to pure Si. The presence of pure Si is probably due to ion sputtering of the substrate during the deposition.

Table 4.1. Elemental composition based on XPS analysis

Element	Line	Percentage
Na	1s	0.07
F	1s	0.16
O	1s	16.9
N	1s	9.7
Ca	2p	0.36
C	1s	59.3
Ar	2p	0.35
Si	2p	13.1

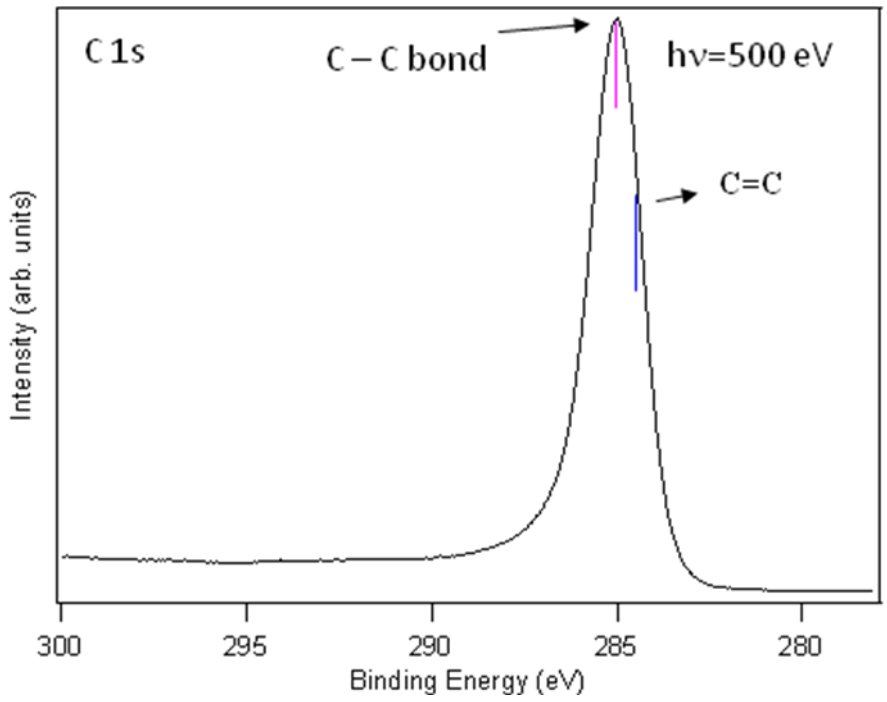

Figure 4.10. XPS spectrum of C 1s in NDLC

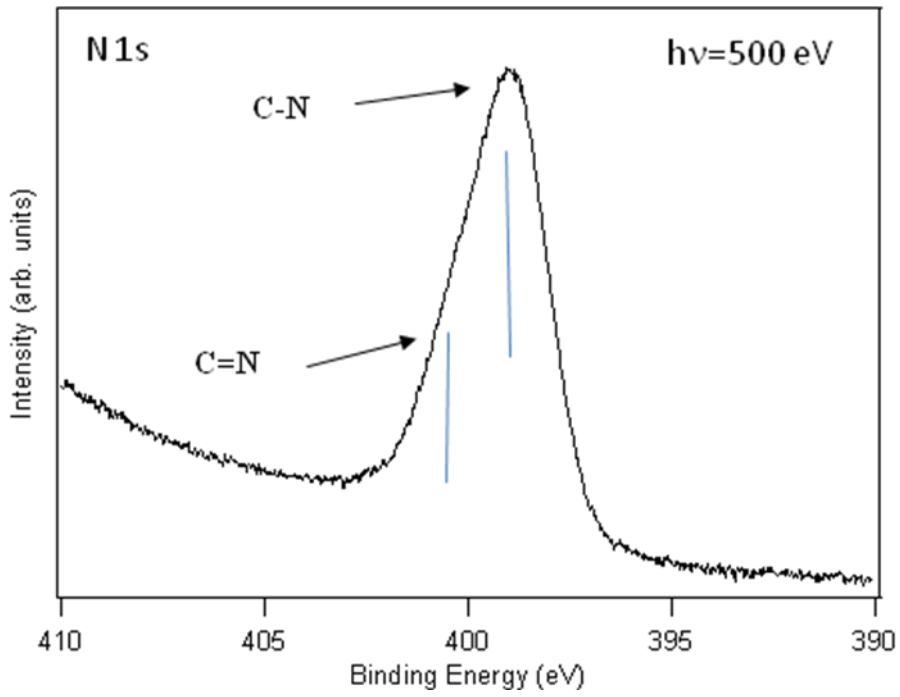

Figure 4.11. XPS spectrum of N1s in NDLC

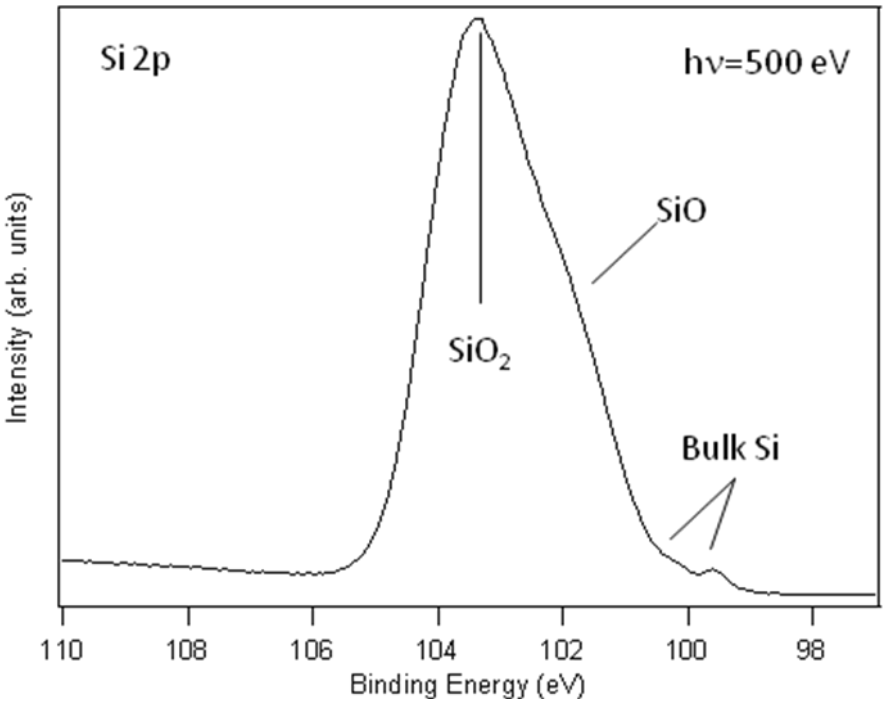

Figure 4.12. XPS spectrum of Si 2p coated with NDLC

4.4 Mechanical Properties

The data of hardness and elastic modulus value are the average values from indentation testing at different locations and are presented in Figures 4.13 - 4.14. The average nanohardness of DLC coated on Si wafers was 18 GPa, whereas that of NDLC is 21 GPa at 45 mN load. It is generally accepted that the hardness of the DLC films have a close relationship with their sp^3/sp^2 ratio, That is, the higher sp^3/sp^2 ratio, the higher the hardness. The lower hardness value of DLC comparing to diamond is due to the existence of sp^2 carbon and hydrogen in the DLC films (Robertson, 1992). From several published results, the doping of nitrogen leads to higher sp^2 content thus lower hardness (Liu *et al.,* 1999). It is reasonable that the doping of nitrogen in this study increased the hardness of the film, because there is no obvious change of the sp^2 content in the films as shown in the Raman spectrum in Figure 4.2. The higher hardness of NDLC is probably due to the effect of doping nitrogen into film.

The hardness value during the measurement is not affected by the hardness value of the substrate, as long as the indentation depth is limited to within 10% of the total film thickness, whereas the measurement of Young's modulus is uncertain and needs certain degree of modeling. If the tip penetration is deeper than 10 % of the thickness of film, the hardness of the substrate will influence the hardness measurement value.

Liu *et al.,* 1999 reported that at low nitrogen contents, nitrogen doping results in forming N_4^+ configuration in the tetrahedral networks without changing the bonding state of carbon whereas high levels of nitrogen results in graphitization of the films, which leads to low hardness and low modulus of the thin films.

Coefficient of friction was determined with reciprocal pin-on-disc testing at normal ambient air, where chrome steel pin was slid on the films, coated on Si substrates. The load was increased gradually from 50 g to 500 g and the friction coefficient obtained for different conditions of films are shown in Figure 4.15. Friction coefficients (COF) were 0.07 and 0.09 for DLC and low concentration of nitrogen doping, respectively. However, the COF was high as nitrogen concentrations were increased to 5 sccm. Low COF obtained on our samples is consistent with the COF value in the work of Won Seok Choi *et al.*, 2007. Low friction coefficient and low wear rates for low nitrogen content films were also reported by Koskinen *et al.*, 1996.

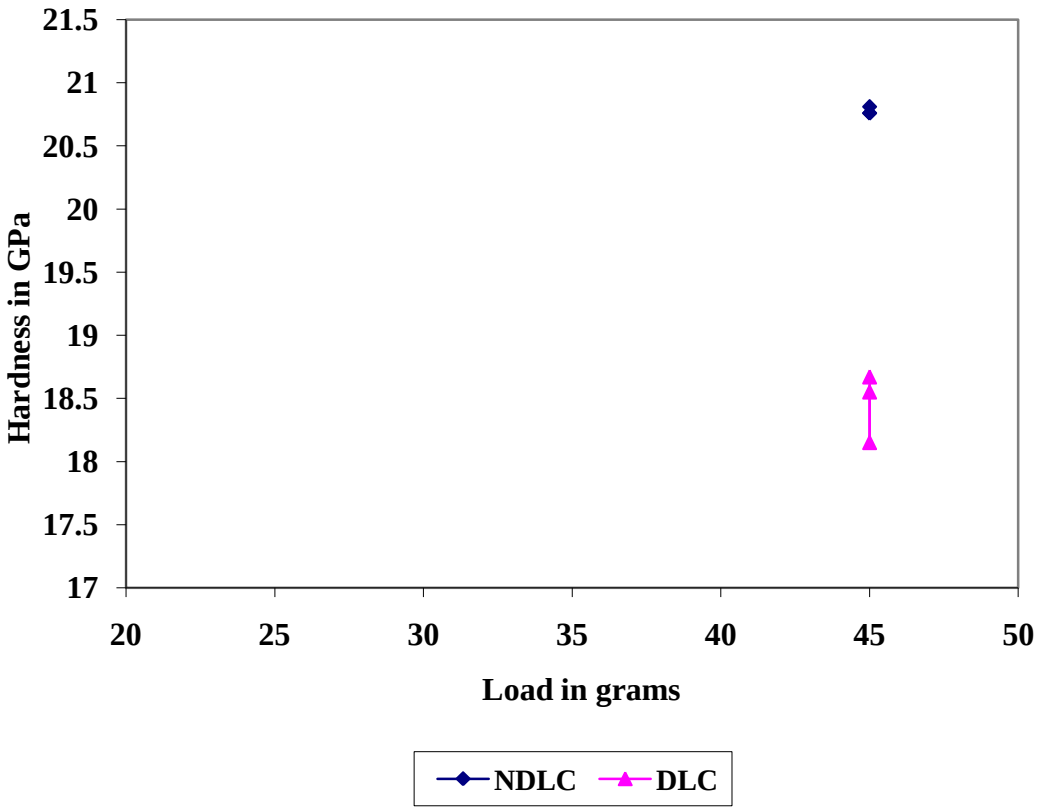

Figure 4.13. Nanohardness of DLC and NDLC

Critical loads for the films were also obtained by acquiring the acoustic emission values in scratch testing. The emission levels jumped to 100% as there was delamination of the films. The results are shown in Figure 4.16. The critical load for DLC, NDLC, and 5-NDLC films is 3.5 N,

3.75 and 2.0 N, respectively. The results indicate that low nitrogen doping increases the adhesion of the film but higher doping concentration decreases the film adhesion.

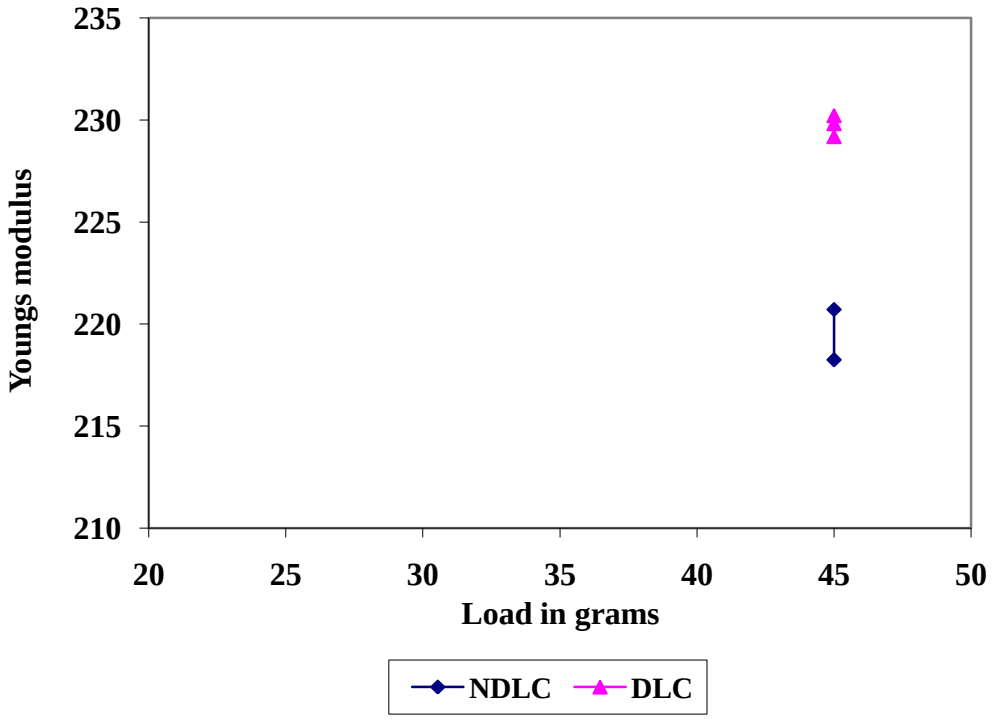

Figure 4.14. Young's modulus of DLC and NDLC

4.5 Surface Energy

Elements like silicon, fluorine, oxygen and nitrogen influence the contact angle. Fluorine has a great influence in polymers and PTFE and is reported to reduce surface energies to as low as 18mN/m (Grischke and Hieke *et al.,* 1997). The contact angle of extruded PTFE used in our study was 89° and the surface energy was 75mN/m. Any increase in the concentration of these elements in the DLC network changes the contact angle of water. Nitrogen, hydrogen and oxygen were reported to reduce the contact angle and increase the surface energy of DLC coating (Wen *et al.,* 2008).

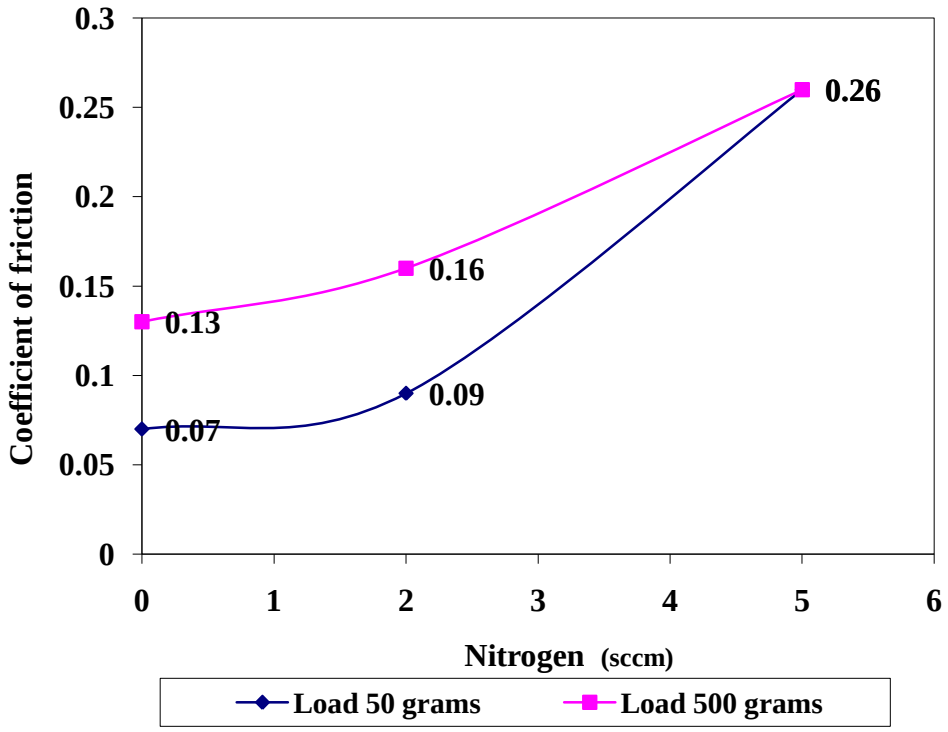

Figure 4.15. Coefficient of friction of thin films

The contact angle on DLC coated PTFE increased to 130° on DLC. Nitrogen doping decreased the contact angle to 111° and thus increased the surface energy to 47mN/m from 27mN/m. The decrease in contact angle and increase in the surface energy corresponds to the decrease in the fluorine content and increase in the nitrogen functional group. The decrease of fluorine and increase of strong nitrogen polar functional group such as C—N, C=N and C_N_F group on PTFE surface contributes to the increase of the surface energy (Chen Jie-Rong *et al.*, 1997).

Surface roughness has a major effect on the contact angle of DLC, as the drop gets pinned on the surface. The contact line of the water droplet can have a complex shape due to the surface geometry and chemical heterogeneity and has an effect on the contact angle (K.Ozeki and K.K.Hirakuri, 2007). The contact angles reported in the literature for DLC are typically in the

range of 70° - 80° (Mirjami Kiuru and Esa Alakoski, 2004). We obtained contact angle of 130° by coating DLC on PTFE.

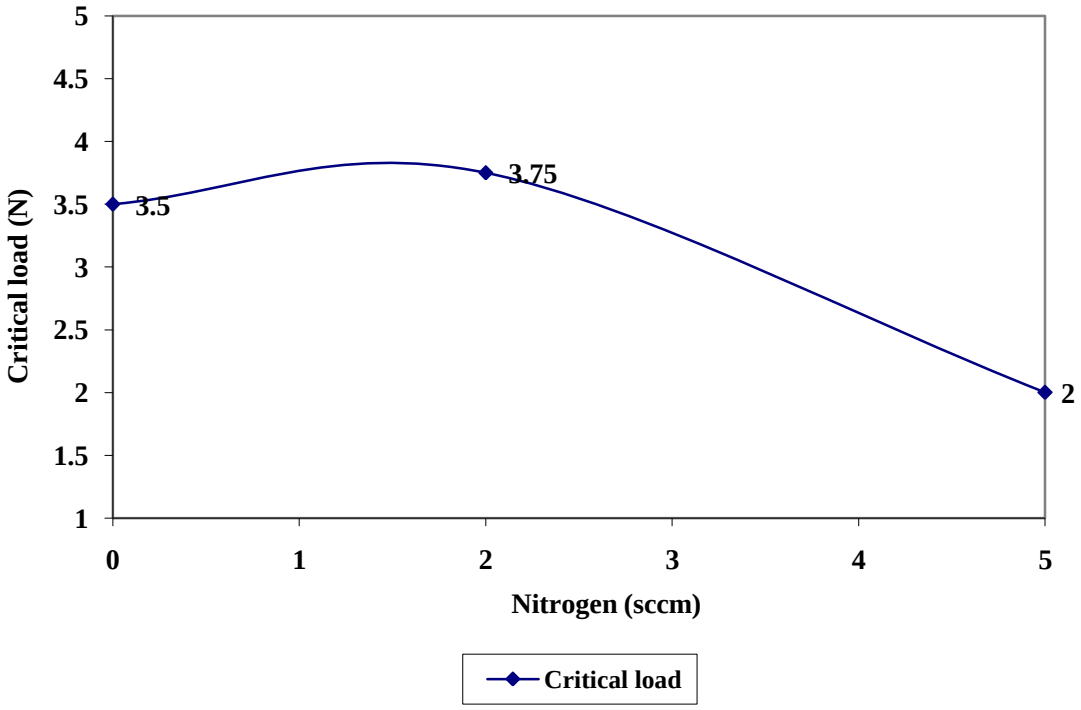

Figure 4.16. Critical load of thin films

Surface energy results obtained for various conditions are reported in Table 4.2. The contact of water droplets on PTFE are shown in Figure 4.17.

Table 4.2. Contact angle and surface energy of DLC coatings

	Contact angle (Degrees)		Surface energy (mN/m)
PTFE	89	88	75
DLC PTFE	124	135	27
NDLC PTFE	113	109	47

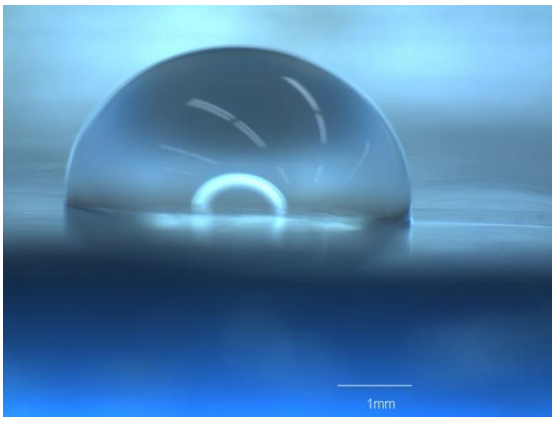

(a)

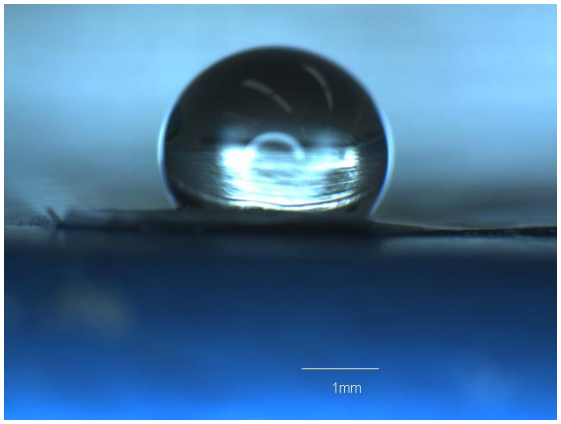

(b)

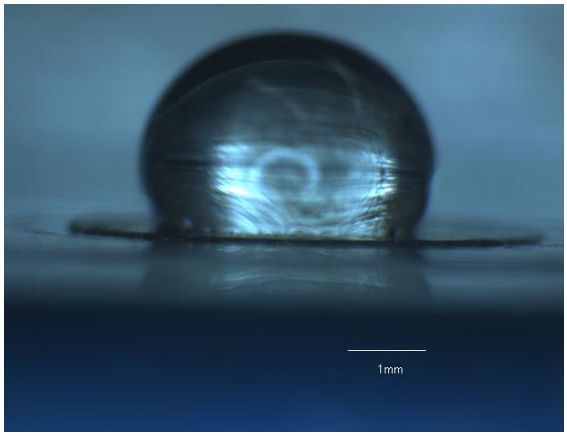

(c)

Figure 4.17. Contact angles on various conditions of PTFE

(a) Uncoated PTFE, (b) DLC coated PTFE, (c) NDLC coated PTFE

4.6 Biocompatibility

4.6.1 Platelet adsorption and activation

Results of adsorbed platelets counted on the DLC coated PTFE surface is shown in Figure 4.18. From this figure it is clear that the number of platelets adsorbed on the coated surface is higher than that on the bare PTFE.

Data expressed in Table 4.3 are platelets adsorbed in each disc of PTFE. Two experiments of platelet adsorption were carried out for 15 and 60 minutes and they were performed by washing the disks with 1 vol.% SDS.

SEM micrographs showing the results of platelets activation are presented in Figures 4.19-4.21. It can be clearly seen from these micrographs that the total number of platelets adhered is different among the three samples. More platelets adhered to the DLC and NDLC coated PTFE disks than bare PTFE. But the platelets on coated surface were much less aggregated and much less activated. There are less platelets adhered to the virgin PTFE. However, these platelets are highly aggregated and activated.

The degree of aggregation and activation was analyzed from the morphology of the platelets adhered. Adhesion of platelets is believed to run in four stages and can be classified as:

(1) Single non-activated

(2) Slightly activated

(3) Spread

(4) Aggregated (two or more aggregates)

Most of the platelets adhered to bare PTFE are aggregated in groups of two or more as shown in Figure 4.19. Highly activated platelet is also shown in Figure 4.19a whereas, most of the platelets on DLC coated PTFE are single and spread and only a few platelets are activated, as shown in Figure 4.20. On the contrary, only single non-spread platelets are seen on the nitrogen-doped DLC surfaces as shown in Figure 4.21. The results show that the NDLC can improve haemocompatibility of PTFE.

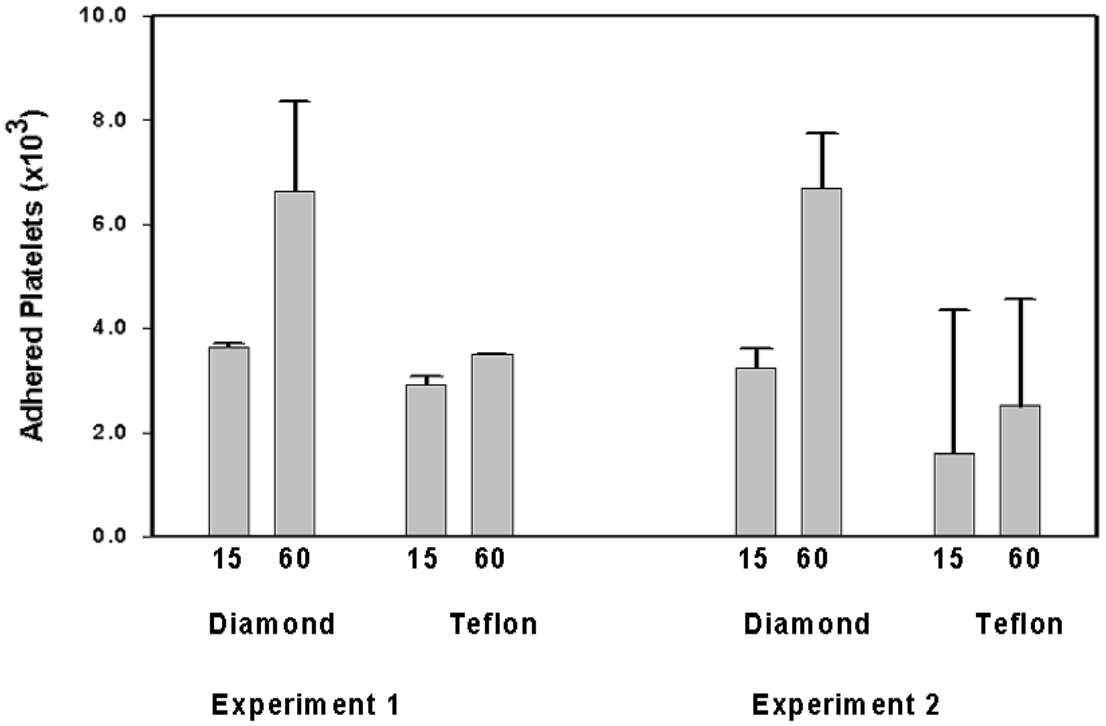

Figure 4.18. Results of radio labelled platelet adsorption

Table 4.3. Summary of platelets adsorbed

	Diamond like carbon		PTFE	
	15 Min	**60 Min**	**15 Min**	**60 Min**
Experiment 1				
Mean	3627	6633	2911	3503
St dev	83	1734	16	2.9
Experiment 2				
Mean	3227	6683	1587	2505
St dev	366	1055	2776	2058

Figure 4.19. Platelets on bare PTFE

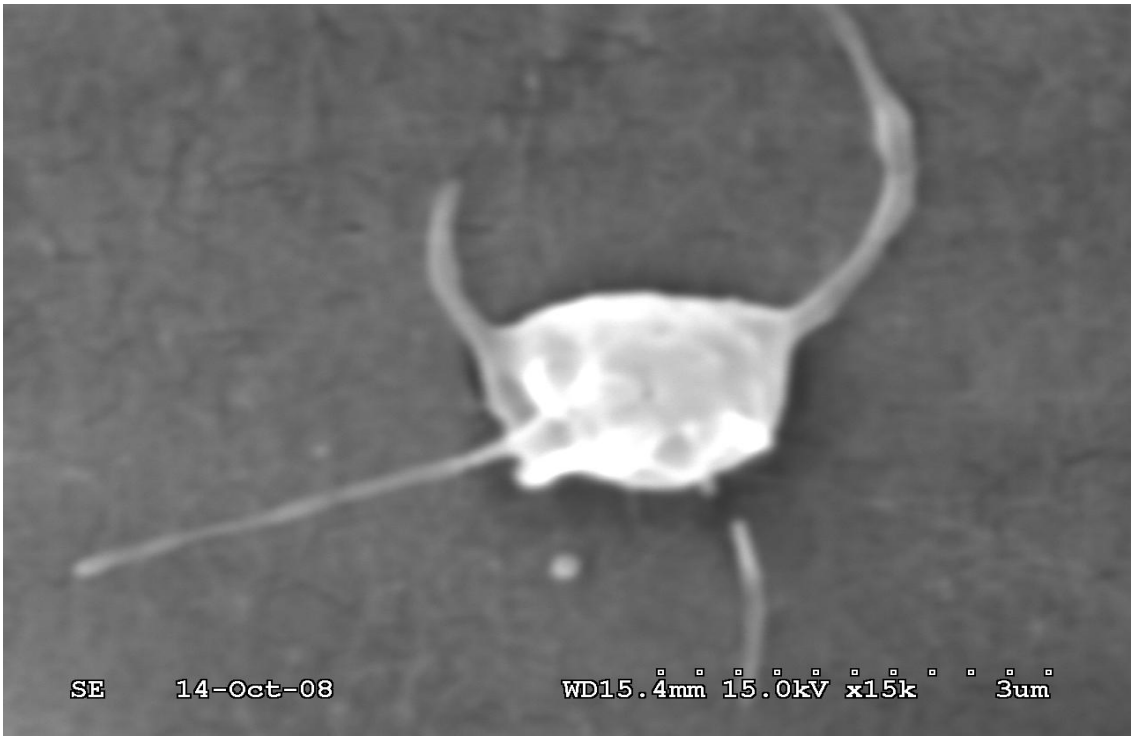

Figure 4.19a. Platelet activated on bare PTFE

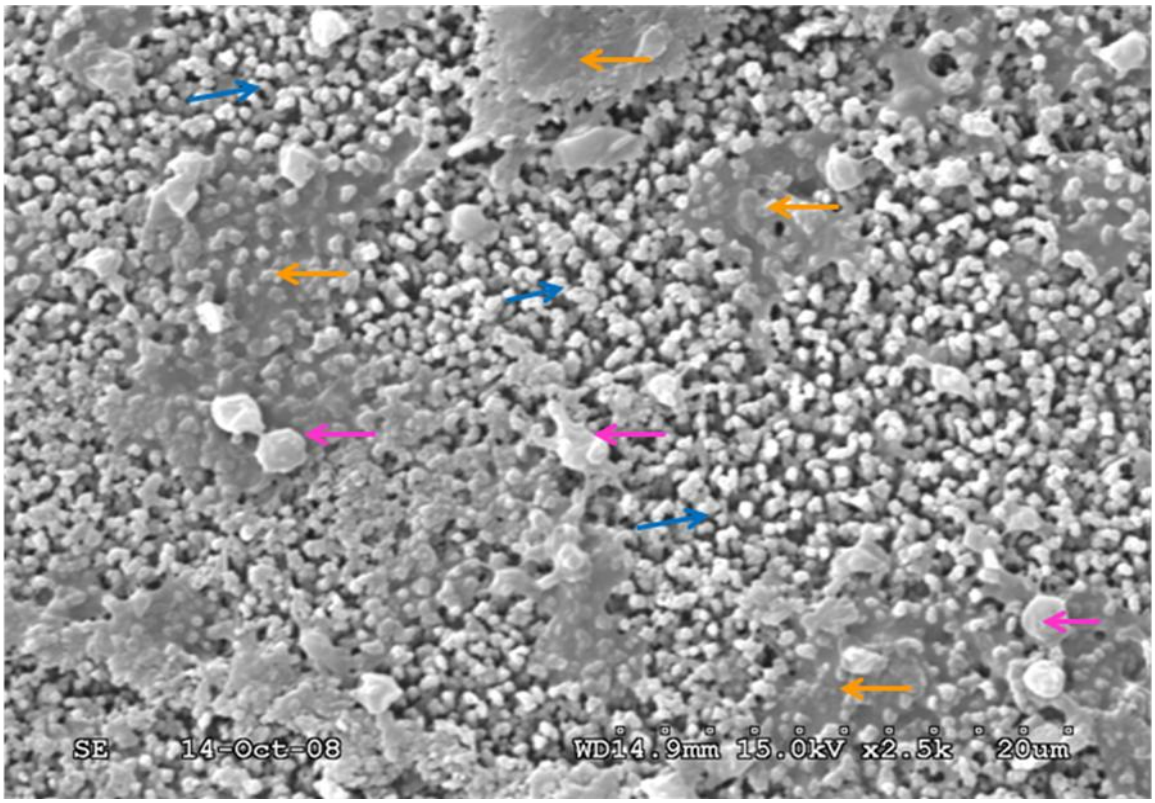

Figure 4.20. Platelets on DLC coated PTFE

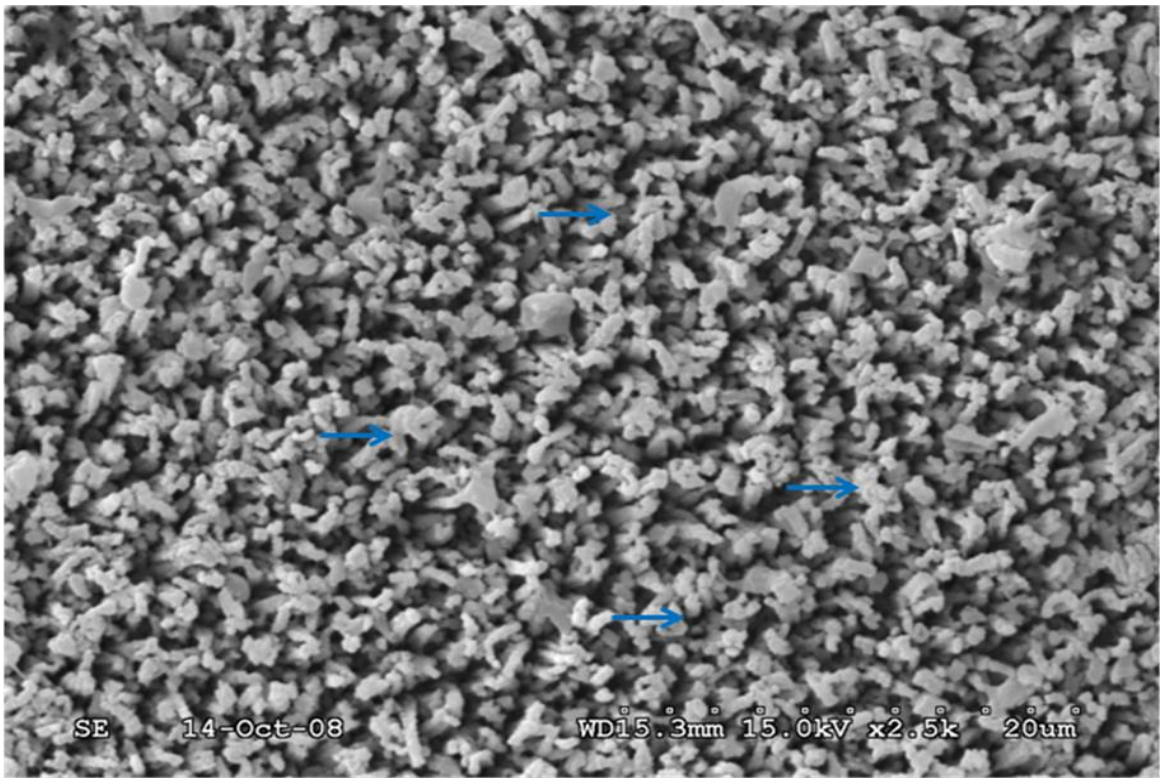

Figure 4.21. Platelets on NDLC coated PTFE

CHAPTER 5

CONCLUSIONS AND FUTURE WORK

Diamond-like carbon thin films were successfully deposited on to silicon and PTFE substrates using ion beam deposition technique with a mixture of Argon and Methane gases. The results are concluded as follows:

1. Ion beam deposited films showed very smooth surface, exhibited high adhesion to the substrate as revealed by critical loads, and low coefficient of friction.

2. Nitrogen was successfully doped into DLC in concentrations up to 10% to form nitrogenated diamond like carbon as analyzed by X-ray photo emission spectroscopy.

3. Nanohardness measurements showed that the low concentrations of nitrogen doping in DLC improved film adhesion without decreasing the hardness.

4. Ion beam deposition of both DLC and NDLC coatings on PTFE increased the surface roughness of PTFE; however, nitrogen doping decreased the roughness of DLC.

5. Both DLC and NDLC coatings increased the water contact angle of PTFE, thus lowering the surface energy and improving the wettability of PTFE; however, nitrogen doping decreased the water contact angle of DLC, thereby increasing the surface energy of DLC.

6. Blood platelet adhesion and reaction shows that both DLC and NDLC increased platelet adsorption but decreased platelet reaction, thus improving the haemocompatibility of PTFE. Nitrogen doping further reduced platelet reaction and improved haemocompatibility of DLC coatings.

The results have demonstrated that DLC coatings, especially NDLC coatings, are able to improve the mechanical and biological performance of PTFE.

Although the results obtained in the recent work strongly suggest that DLC coating by IBD improves the haemocompatibility of PTFE, further studies on the effect of nitrogen concentration and carbon structure on the biocompatibility is desirable to have a deep understanding of the relationships between the structure and biomedical properties of the DLC thin films.

LIST OF REFERENCES

Abrasonis, G., Gayo, R., Vinnichenko, M., Kreissig, U., Kolitsch, A., and Moller,W. (2006). Sixfold ring clustering in sp2-dominated carbon and carbon nitride thin films a Raman spectroscopy study. *Physical Review*, B73, 125427.

Aisenberg, S., Chabot, R., Ion-beam deposition of thin films of diamond-like carbon. (1971). *Journal of Applied Physics*, 42 (7), 2953-2958.

Aisenberg & Kimock, F.M. (1990). Properties and characterization of amorphous carbon coatings. *Materials Science Forum*, 52-53, 1-39.

Angus, J.C., Hayman, C.C. (1988). Low-pressure, metastable growth of diamond and diamond like phase. *Science*, 241, 913-921.

Angus, J.C., Wang, Y. (1991). *Diamond and Diamond-like films and Coatings*, edited by Clausing, R.E., Angus, J.C., Horton, L.L., Koidl, P. (1991). Springer-Voriag, New york LLC, 173.

Ali Erdemir., Christophe Donnet. (2006). Tribology of diamond-like carbon films: recent progress and future prospects. *Journal of Applied Physics. D*, 39, R311 – R327.

Baba, K., Hatada, R. (2006). Deposition of diamond like carbon films on polymers by plasma source ion implantation. *Thin Solid Films*, 506-507, 55-58.

Black, J. (1999). Biological performance of materials: Fundamentals of biocompatibility. New York: Marcel Dekker.

Bourgoin, D., Turgeon, S., Ross, G.G. (1999). Characterization of hydrogenated amorphous carbon films produced by plasma-enhanced chemical vapor deposition with various chemical hybridizations. *Thin Solid Films*, 357, 246-253.

Casiraghi, C., Ferrari, A.C., & Robertson, J. (2005). Raman spectroscopy of hydrogenated amorphous carbons. *Physical Review*, B 72, 085401.

Chen Jie-Rong., Wakida, T. (1998). Studies on the surface free energy and surface structure of PTFE film treated with low temperature plasma. *Journal of Applied Polymer Science*, 63 (13), 1733-1739.

Courtney, J.M., Lamba, N.M.K., Sundaram, S., and Forbes, C.D. (1994). Biomaterials for blood-contacting applications. *Biomaterials*, 15 (10), 737-744.

Cui, F.Z., Li, D.J. (2000). A review of investigations on biocompatibility of diamond-like carbon and carbon nitride films. *Surface & Coatings Technology*, 131, 481-487.

Cuomo, J.J., Pappas, D.L., Bruley, J., Doyle, J.P., Saenger, K.L. (1991). Vapor deposition processes for amorphous carbon films with sp3 fractions approaching diamond. *Journal of Applied Physics*, 70, 1706.

Debdulal Roy., Manish Chhowalla., Niklas Hellgren., Clyne, T.W., & Amaratunga, G.A.J.(2004). Probing carbon nanoparticles in CNx thin films using Raman spectroscopy. *Physical Review*, B70, 035406.

Erdeimer, A., Donnet, C. (2001). Tribology of diamond, diamond-like carbon and related films. *In modern tribology handbook*, Edited by Bhushan, CRC press, Boca Ralton, FL, 2, 871-906.

Ferrari, A.C., Robertson, J., Interpretation of Raman spectra of disordered and amorphous carbon. (2000). *Physical Review*, BV61, 20.

Field, J.E. (1993). Properties of Diamond. *Academic Press*, London.

Foursa, M., Plasma- assisted deposition of nitrogen doped amorphous carbon films onto polytetrafluroethylene for biomedical applications. (2007). Ph.D *Thesis*, University of Saskatchewan.

Geoffrey Dearnaley., James H, Arps. (2005). Biomedical applications of diamond-like carbon (DLC) coatings: A review. *Surface & Coatings Technology*, 200, 2518-2524.

Grischke, M., Hieke, A., Morgenweck, F., Dimigen, H. (1998). Variation in wettability of DLC-coatings by network modification using silicon and oxygen. *Diamond and Related Materials*, 7, 454-458.

Hasebe, T., Ishimaru, T., Kamijo, A., Yoshimoto, Y., Yoshimura, T., Yohena, S., Kodamaa, H., Hotta, A., Takahashi, K., Suzuki, T. (2007). Effects of surface roughness on anti-thrombogenicity of diamond-like carbon films. *Diamond & Related Materials*, 16, 1343-1348.

Hellgren, N., Johansson, M.P., Broitman, E., Hultman, L., Sundgren, J.E. (1999). Role of nitrogen in the formation of hard and elastic CN_x thin films by reactive magnetron sputtering. *Physical Review B,* 59, 5162-5177.

Huang Yana, Lu., Xiaoyinga., Ma Jingwu a., Huang Nanb. (2008). In vitro investigation of protein adsorption and platelet adhesion on inorganic biomaterial surfaces. *Applied Surface Science*, 255, 257-259.

Ikada, Y. (1994). Surface modification of polymers for medical applications. *Biomaterials*, 15 (10), 725-736.

Irmer, G., & Dorner-Reisel, A. (2005). Micro-Raman Studies on DLC Coatings. *Advanced Engineering Materials*, 7 (8), 694-705.

Jiehe Sui & Wei Cai. (2001). Mechanical properties and anti-corrosion behavior of the diamond-like carbon films. *Surface and Coatings Technology*, 3-4, 1323-1327.

Junying Hao., Weimin Liu., Qunji Xue. (2007). Effect of N2/CH4 flow ratio on microstructure and composition of hydrogenated carbon nitride films prepared by a dual DC-RF plasma system. *Journal of Non-Crystalline Solids*, 353, 136-142.

Kaufman,H. (1990). Broad beam ion sources. *Rev. Science Instrum*, 61, 230.

Kelly, B.T. (1981). Physics of Graphite. *Applied Science Publishers*, London.

Kimock, Fred, D.M., David W, Brown., Steven J. Finke & Edward G. Thear. *Diamonex, Inc, Allentown, PA, USA, data tech*, 69-76.

Koidl, P., Wild, Ch., Dischler, B., Wagner, J., Ramsteiner, M. (1990) Properties and Characterization of Amorphous Carbon Films. *Materials Science Forum*, 52 (53), 41-70.

Koskinen, J.P., Hirvonen, J., Levoska and P. Torri. (1996). Tribological characterization of carbon-nitrogen coatings deposited by using vacuum arc discharge. *Diamond and Related Materials*, 5, 669-673.

Kusano, Y., Evetts, J.E., Somekh, R.E., and Hurchings, I.M. (1998). Properties of carbon nitride films deposited by magnetron sputtering. *Thin Solid Films*, 332, 56-61.

Lifshitz, Y. (1999). Diamond-like carbon- Present status. *Diamond and Related Materials*, 8, 1659-1676.

Lifshitz, Y., Kasi, S.R., & Rabalis, J.W. (1990). Subplantation model for film growth from hyperthermal species. *Physical Review B*, 41 (15), 10468-10480.

Liu.E, X.Shi., H.S.Tan., L.K.Cheah., Z.Sun., Tay, B.K., Shi, J.R. (1999). The effect of nitrogen on mechanical properties of tetrahedral amorphous carbon films deposited with a filtered cathodic vacuum arc. *Surface and Coatings Technology*, 120 -121, 601-606.

Liu, A.Y., Cohen, M.L. (1990). Structural properties and electronic structure of lowcompressibility materials-beta Si3N4 and hypothetical beta-C3N4. *Physical Review B*, 41, 10727-10734.

McKenzie, D.R., Mcphedran, R.C., Savvides, N., Botten, I.C. (1983). Properties and structure of amorphous hydrogenated carbon films. *Philosophical Magazine B*, 48, 341-364.

Merel, P., Tabbal, M., Chaker, M., Moisa, S., Margot, J. (1998). Direct evaluation of the sp^3 content in diamond-like-carbon films by XPS. *Applied Surface Science*, 136, 105-110.

Mirjami Kiuru., Esa Alakoski. (2004). Low sliding angles in hydrophobic and oleophobic coatings prepared with plasma discharge method. *Materials Letters*, 58, 2213-2216.

Moulder *et al*., (1995). Handbook of X-ray Photoelectron Spectroscopy. *Physical Electronics Inc*.

Narayan. Roger, J. (2005). Nanostructured diamond-like carbon thin films for medical applications. *Material Science and Engineering*, C25, 405-416.

Ozeki, K & Hirakuri, K.K. (2008). The effect of nitrogen and oxygen plasma on the wear properties and adhesion strength of the diamond-like carbon film coated on PTFE. *Applied Surface Science*, 254 (6), 1614-1621.

Pharr, G.M., Callahan, D.L., McAdams, S.D., Tsui, T.Y., Anders, S., Anders, A., Ager III, J.W., Robertson, J. (1996) . Hardness, elastic modulus and structure of very hard carbon films produced by cathodic-arc deposition with substrate pulse biasing. *Applied Physics Letters*, 68 (6), 779-781.

Prioli, S.I., Zanette, A.O., Caride, D.F., Franceschini & Freire Jr, F.L. (1996). Atomic force microscopy of amorphous hydrogenated carbon–nitrogen films deposited by radiofrequency-

plasma decomposition of methane–ammonia gas mixtures. *Journal of Vacuum Science and Technology A,* 14, 2351-2355.

Robertson, J. (1986). Amorphous carbon. *Advances in Physics*, 35, 317-374.

Robertson, J. (1993). Deposition mechanisms for promoting sp3 binding in diamond-like carbon. *Diamond and Related Materials*, 2, 984-989.

Robertson, J. (2002). Diamond-like amorphous carbon. *Materials Science and Engineering R*, 37, 129-281.

Roy, P.K., Choi, H.W., Yi, J.W., Moon, M-W., Lee, K-R., Han, D.K., Shin, J.H., Kamijo, A., Hasebe, T. (2009). Hemocompatibility of surface–modified, silicon-incorporated, diamond–like carbon films. *Acta Biomaterialia*, 5, 249-256.

Silva, S.R.P., Amaratunga, G. (1994). Use of space-charge-limited current to evaluate the electronic density of states in diamond-like carbon thin films. *Thin Solid Films*, 253, 146.

Srinivasan, S., Yang, Q. (2007). Nitrogen Doped Diamond like Carbon Thin Films for Enhanced Biological Properties. *Proceedings of the 2007 Joint International Conference of the 3rd International Conference on SISE and SEIA*, 1-8

Takadoum, J., Raunch, J.Y., Cattenot, M.J., Martin, N. (2003). Comparative study of mechanical and tribological properties of CNx and DLC films deposited by PECVD technique. *Surface and Coatings Technology*, 74-175, 427-433.

Tirrell, M., Kokkoli, E., Biesalski, M. (2002). The role of surface science in bioengineered materials. *Surface Science,* 61–83.

Vasilets, V.N., Hirose, A., Yang, Q., Singh, A., Sammynaiken, R., Shulga, Yu.M A., Kuznetsov, V., Sevastianov, V.I. (2005). Hot-wire plasma deposition of doped DLC films on fluro carbon polymers for biomedical applications. *Plasma Processes and Polymer*s, 65-76.

Weiler, M., Sattel, S., Jung, K., Ehrhardt, H., Veerasamy, V.S., Robertson, J. (1994). Highly tetrahedral, diamond-like amorphous hydrogenated carbon prepared from a plasma beam source. *Applied Physics Letters*, 64 (21), 2797-2799.

Wena, F., Huang, N., Leng, Y.X., Zhao, A.S., Jing, F.J. (2008). Study on wettabilities and platelet adhesion behavior of C:H and C:N:H films prepared by DC-MFCVA. *Applied Surface Science* , 255, 469–472.

Wilmer Sucasine., Masco matsuoka., Karina C.Lopes *et al*. (2006). Raman and Infrared spectroscopy studies of carbon nitride films prepared on Si (100) substrates by ion assisted deposition. *J.Braz, Chem Soc*, 17 (6), 1163-1169.

Won Seok Choi ., Mungi Park ., Byungyou Hong. (2007). An examination of trace surface on diamond-like carbon film after ball-on disk measurement *Thin Solid Films*, 515, 7560-7565.

Xiaoming He., Wenzhi Li., and Hengde Li. (1996). Diamond-like carbon film synthesized by ion beam assisted deposition and its tribological properties. *Journal of Vacuum Science and Technology.* A, 14(4), 2039-2047.

Yeh, J.-J., Lindau, I. (1985). Atomic subshell photoionization cross sections and asymmetry parameters: 1 < Z < 103. *At. Data Nucl. Data Tables*, 32, 1.

Zheng, C.L., Cui, F.Z., Meng, B., Ge, J., Liu, D.P., & Lee, I-S. (2005). Hemocompatibility of C-N films fabricated by ion beam assisted deposition. *Surface and Coatings Technology*, 193(1-3), 361-365.

Ziegler, J.F., Biersack, J.P., Littmark, U. (1985). The Stopping and Range of Ions in Solids. *Pergamon Press, Oxford*.